

REPORT DOCUMENTATION PAGE			<i>Form Approved</i> <i>OMB No. 0704-0188</i>	
Public reporting burden for this collection of information is estimated to average 1 hour per response, including the time for reviewing instructions, searching existing data sources, gathering and maintaining the data needed, and completing and reviewing this collection of information. Send comments regarding this burden estimate or any other aspect of this collection of information, including suggestions for reducing this burden to Department of Defense, Washington Headquarters Services, Directorate for Information Operations and Reports (0704-0188), 1215 Jefferson Davis Highway, Suite 1204, Arlington, VA 22202-4302. Respondents should be aware that notwithstanding any other provision of law, no person shall be subject to any penalty for failing to comply with a collection of information if it does not display a currently valid OMB control number. PLEASE DO NOT RETURN YOUR FORM TO THE ABOVE ADDRESS.				
1. REPORT DATE (DD-MM-YYYY) 30-04-2010		2. REPORT TYPE Final		3. DATES COVERED (From - To) 01 May 2009 - 30 Apr 2010
4. TITLE AND SUBTITLE Plasma Reforming of Liquid Hydrocarbon Fuels in Non-Thermal Plasma-Liquid Systems			5a. CONTRACT NUMBER	
			5b. GRANT NUMBER EOARD 088001	
			5c. PROGRAM ELEMENT NUMBER	
6. AUTHOR(S) Prof. Chernyak, Valeriy			5d. PROJECT NUMBER STCU P354	
			5e. TASK NUMBER #T04	
			5f. WORK UNIT NUMBER	
7. PERFORMING ORGANIZATION NAME(S) AND ADDRESS(ES) Kiev National Taras Shevchenko University Faculty of Radio Physics Prospect Acad. Glushkova 2/5 Kyiv 03022, Ukraine			8. PERFORMING ORGANIZATION REPORT N/A	
9. SPONSORING / MONITORING AGENCY NAME(S) AND ADDRESS(ES) EOARD PSC 802 Box 14 FPO 09499-0014 223 Old Marylebone Road London, NW1 5TH, UK Stephanie Masoni			10. SPONSOR/MONITOR'S ACRONYM(S) AFOSR/NA 875 Randolph St. Suite 325, Room 3112 Arlington, VA 22203 USA	
			11. SPONSOR/MONITOR'S REPORT NUMBER(S) STCU P354	
12. DISTRIBUTION / AVAILABILITY STATEMENT Approved for public release, unlimited distribution				
13. SUPPLEMENTARY NOTES				
14. ABSTRACT The report results from the project tasking the researchers from the Kiev National Taras Shevchenko University under the STCU-EOARD-AFOSR Partner Program to study new methods of low-temperature plasma-enhanced reforming of liquid hydrocarbon bio-fuels in non-thermal plasma-liquid electric discharge systems for applications in prospective fuel-flexible plasma-assisted combustion technologies. The research program includes four research stages: (1)preparation of modules of plasma-chemical reactors for plasma reforming of liquid fuels by the electric discharge in a gas channel with liquid wall; (2)examination and characterization of gas-liquid discharge systems and processes of plasma reforming of liquid fuels using methods of optical emission/absorption spectroscopy, gas chromatography, mass spectrometry and others; (3)study of regimes of plasma reforming of model fuel mixtures in gas-liquid discharge systems using numerical modeling and simulation together with experimental diagnostics; and (4)analysis and synthesis of research data and preparation of recommendations for its applications. This is a final progress report of research activity.				
15. SUBJECT TERMS EOARD, non-thermal plasma chemistry, dynamic electric discharge gas-liquid system, hydrocarbon liquid fuels, plasma fuel reforming				
16. SECURITY CLASSIFICATION OF:			17. LIMITATION OF ABSTRACT UL	18. NUMBER OF PAGES 49
a. REPORT UNCLASS	b. ABSTRACT UNCLASS	c. THIS PAGE UNCLASS		
			19b. TELEPHONE NUMBER (include area code) (703) 696-8478	

**Progress Report
for STCU-EOARD Project P354**

**Plasma Reforming of Liquid Hydrocarbon Fuels
in Non-Thermal Plasma-Liquid Systems**

for the period 1 May 2009 – 30 April 2010

**by Prof. V.Ya. Chernyak
Kiev National Taras Shevchenko University**

CONTENTS

1.	Summary	3
2.	Introduction	4
3.	Methodology	6
4.	Results	7
4.1.	Experimental Setups	7
4.2.	Diagnostic methods	9
4.3.	Numerical models	19
4.4.	Modeling of dusty plasmas with liquid microparticles	20
4.5.	Results and discussion	21
5.	Conclusions	44
6.	Acknowledgements	46
7.	References	47
8.	Abbreviations	49

SUMMARY

The project tasking researchers from the Radio-Physical Faculty of Kyiv National Taras Shevchenko University in the framework of the STCU-EOARD-AFOSR Partner Program is addressed to investigations in the field of physics and chemistry of plasma-assisted combustion with the aim of development of novel methods of non-thermal plasma-chemical reforming of liquid hydrocarbon bio-fuels for applications in fuel-flexible plasma-supported combustion technologies. The fundamentals for proposed approaches are grounded on unique features of gas-liquid electric-discharge systems and advantageous of non-equilibrium chemically reacting plasmas. The main ideas are related to possibilities of cost-effective non-thermal plasma-chemical fuel reforming and more efficient usage of hydrogen-rich bio-fuels. The project is based on existing achievements in physics and chemistry of dynamic electric-discharge plasma-liquid systems, which have priority character. The model bio-fuel under study is ethanol-water mixture. The plasma-forming gas is atmospheric air. As a source of non-thermal plasma, the electric discharge in a gas channel with liquid wall is used. Research involves experimental and theoretical studies with the use of special methods of diagnostics of electric discharge plasma and liquid fuel, including optical emission spectroscopy, mass spectrometry, gas chromatography and calorimetry as well as numerical modeling and simulation. The results are new data on properties of non-equilibrium plasma in heterogeneous gas-liquid systems; characteristics of plasma reforming of ethanol-water mixtures in plasma-chemical reformers with the electric discharge in a gas channel with liquid wall; evaluation of potential enhancement of plasma reforming of real fuels and recommendations to its implementation in prospective aerospace plasma-assisted combustion technologies.

INTRODUCTION

Combustion efficiency plays a critical role in performance of chemical energy conversion and chemical jet propulsion systems. For this reason, searching of innovative ideas and approaches to efficient combustion is very important for progress toward the development of more advanced combustion technologies.

From physics and chemistry of fuel combustion it is known that addition of light inflammable gases (H_2 , CO) essentially improves ignition/combustion of heavy oil and bio-fuels [1]. Therefore hydrogen is considered as one of the most prospective energy sources for the future that can be renewable, ecologically clean and environmentally safe [2]. Among possible technologies for free hydrogen production, including steam reforming and partial oxidation of bio-fuels [3], a low-temperature plasma-assisted fuel reforming is believed to be a good alternative approach [4,5]. Although the plasma reforming process needs some additional electric power, its potential advantages: fast start-up, easy control, cooking reliability, compact design, etc provide good perspectives in its applications in aerospace technologies. Also the use of fuel reforming can be rather perspective for hypersonic ($M > 5$) aircrafts as will allow to solve two basic tasks: the presence of quickly combustible fuel on board of aircraft and the maintenance of cooling of aircraft systems. The possible approach to the decision of these tasks can be on-board reforming of fuel (for example, kerosene), i.e. its conversion into H_2 and CO_2 : hydrogen can be used for combustion and carbon dioxide - for aircraft cooling purposes. For on-board applications, electric power consumption should be within necessary and sufficient amount available on-board. Therefore, plasma fuel reforming should maximize hydrogen production and minimize power consumption. To optimize the reforming process, the parameters and regimes should be analyzed in terms of hydrogen yield and energy efficiency of reforming.

For plasma fuel reforming, various methods using thermal and non-thermal plasma are known [6]. Thermal plasma, which is thermodynamically equilibrium, has characteristics of high ionization by higher energetic density. This has merits of good rate of fuel decomposition but demerits of poor chemical selectivity and high specific energy consumption. Non-thermal (low-temperature) plasma, which is kinetically non-equilibrium, has characteristics of low ionization but benefits of high reactivity and selectivity of chemical transformations providing high enough productivity at relatively low energy consumption; this can be obtained by high voltage discharging in a flow at low or high atmospheric pressures [7,8].

Among possible types of electric discharges, which can produce non-thermal reacting plasma at high pressures, two specific cases are of research interest of scientists from the Faculty of Radio-Physics in the Kiev National Taras Shevchenko University (KNU). One source is the transverse arc in a blowing flow (BTA) that is an intermediate case of a high-voltage low-current self-sustained discharge with arc length adjusted by the transverse gas flow [9]. It differs from the non-stationary gliding arc of Czernichowski type by the fixed arc length. It also has a convective cooling of the plasma by gas flow without conductive heat losses at the walls since it is a free arc jet. An intensive transverse gas ventilation of the BTA plasma increases its ionization non-equilibrium and non-isothermality [10]. This factor has fundamental importance for plasma-chemical efficiency. Whereas the most of the discharge energy goes into the mean energy of electrons and not just to thermal heating, it gives desirable reactivity and selectivity of chemical

transformations. BTA was tested successfully in the KNU in different variants with the primary and secondary discharges for the plasma processing of various homo- and heterophase gas and liquid substances, including plasma-assisted fuel combustion [11].

Another potential source of non-thermal plasma that can provide simultaneously a high level of non-equilibrium and high density of reacting species in the plasma-liquid system is the electric discharge in a flowing gas channel with liquid wall (DGCLW). Its main properties are [12]: (i) large ratio of the surface of plasma-liquid contact to the plasma volume; (ii) possibility of controlling of plasma-created gas-phase and hetero-phase components, which specifies its potential opportunities during plasma-liquid processing; (iii) possibility of using non-classic liquids including colloidal solutions and mash (waste liquids with fine solid aggregates); (iv) possibility to realize both DC and AC modes of discharge (in contrast with quasi-stationary modes of diaphragm discharges and capillary discharges). DGCLW has been initially realized and investigated in plasma treatment of organics in air-water, phenol and toluene systems [13, 14]. For the purposes of fuel reforming, DGCLW has been proposed in the KNU for the first time at the end of 2006 [15]. The main idea is that DGCLW can be burning directly within the liquid hydrocarbon fuels without preliminary gasification [16]. Another peculiarity is that DGCLW can work in the bubbling microporous liquid which has a very large ratio of the plasma-liquid contact surface to the plasma volume. As is known the ultrasonic (US) cavitation is a very effective method for creating micropores in liquid [17]. Therefore, the DGCLW with additional US pumping is also very interesting for research and development.

The objective of the project is to develop and to study new methods of low-temperature plasma-enhanced reforming of liquid hydrocarbon fuels for applications in prospective plasma-assisted aerospace combustion technologies.

METHODOLOGY

The general technical approach used in the project is based on principles of physics of electric discharge plasma, plasma chemistry and plasma-chemical technology. The specific project approach is in the use of non-equilibrium chemically reactive plasma for low-temperature plasma-chemical processing of liquid hydrocarbon fuels in heterogeneous plasma-liquid systems.

For a case study, the model hydrocarbon fuel is bio-ethanol (ethyl alcohol); the diluting agent is water; the plasma-forming gas is air of atmospheric pressure, the source of non-thermal plasma is the high-voltage electric discharge in the gas channel with liquid wall.

The principal facilities used in the project are:

- dynamic electric-discharge plasma generators;
- plasma-chemical gas-liquid flow reactors of atmospheric pressure;
- high-voltage DC/AC power supply, gas, water and vacuum pump systems;
- electrical measurement instrumentation (digital DC/pulse source meters, oscilloscopes, etc.);
- analytical technique (gas chromatographs, mass-spectrometers, chemical analysis, etc.);
- optical diagnostics (UV-NIR spectrometers, monochromator, lasers, spectral lamps, etc.)
- computer software and numerical codes for data processing, simulation and analysis.

Research program includes experimental and theoretical studies according to goals stated in the introduction. The duration of the project is one year (12 months). According to the program, the work plan consists of four project stages related to four project tasks:

Stage 1 (Quarter 1) => Research on Task #1:

Preparation of laboratory modules of gas-liquid plasma-chemical reactors for non-thermal plasma reforming of liquid fuels using the electric discharge in a gas channel with liquid wall. The expected deliverables are test modules assembly and selected methods of modeling and diagnostics.

Stage 2 (Quarter 2) => Research on Task #2:

Examination and characterization of the process of non-thermal plasma reforming of liquid fuels in the discharge in a gas channel with liquid wall using detailed optical emission/absorption spectroscopic, gas chromatographic, mass spectrometric, and calorimetric diagnostics. The expected deliverables are feasibility demonstration of work process of plasma-liquid fuel reforming and test data on properties of non-equilibrium plasma in the plasma-liquid system using the high voltage discharge in a gas channel with liquid wall.

Stage 3 (Quarter 3) => Research on Task #3:

Experimental study of regimes and parameters of non-thermal plasma reforming of liquid fuels in the discharge in a gas channel with liquid wall using detailed numerical modeling and simulations together with diagnostics. The expected deliverables are optimal parameters and regimes of plasma-chemical reforming of model liquid fuels.

Stage 4 (Quarter 4) => Research on Task #4:

Analysis and synthesis of research data on operation of discharge plasma-liquid systems during liquid fuel reforming; evaluation of the potential of plasma reforming of real fuels, preparation of the final project report; implementation of the project results. The expected deliverables are basic principles and recommendations for applications of new methods of non-thermal plasma-liquid fuel reforming in aerospace fuel-flexible combustion technologies.

RESULTS

Accomplishments in the reporting period

Experimental Setups

The following setups were prepared with the PLS reactors with the DGCLW working with one and two gas streams injected into the homogeneous work liquid as is shown in Fig.1a and Fig.1b. It consists of the cooper rod electrodes (1), plasma column (2), work liquid (3), electrode in liquid (4), and quarts tubes (5). The discharge channel in the work liquid was formed in two ways: with a constant gas flow and without it. As a work gas, we used a standard technical air of atmospheric pressure. As work liquids, we used ethanol, water, and ethanol-water mixtures.

Various modes of the discharge operation were tested: I) the mode where the voltage applied to the electrodes mounted into the lower and upper flanges and the discharge was initiated between them; II) the mode where “+” was applied to the electrode mounted into the lower flange, whereas “-” was applied to the liquid (“liquid” cathode); and III) the mode where “-” was applied to the electrode mounted into the lower flange, while “+” was applied to the liquid (“liquid” anode). Figure 2 shows the dc DGCLW working in the mode I in water.

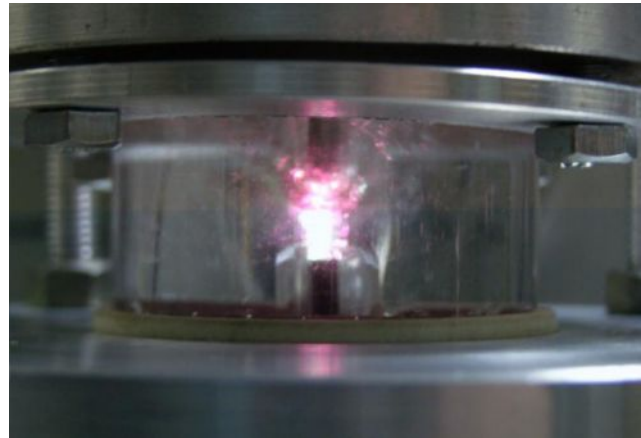
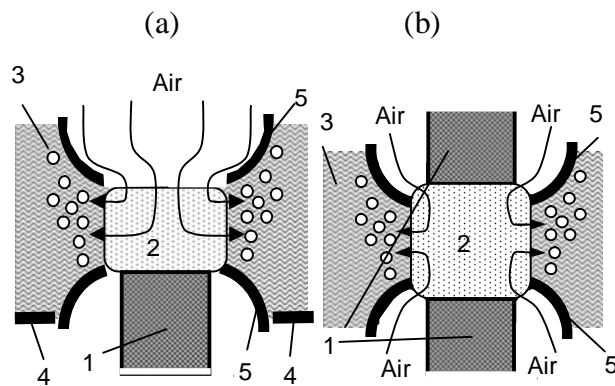


Fig. 1. Schematic of discharge in usual liquid: **(a)** one solid electrode; **(b)** two solid electrodes **Fig. 2.** Photo of discharge at air flow in water. DC DGCLW mode I with two solid electrodes.

Another PLS reactor was prepared with the DGCLW working with the air flow in the liquid under the induced microporous inhomogeneous conditions as is shown in Fig. 3. Here, the airflow was injected into the work liquid (3) through a copper tube (1) covered by a glass insulator (2) and it ran over a flat dielectric surface of the magnetostrictive transmitter (5) which produced ultrasonic (US) cavitations, so the discharge channel (4) was formed by the air flow and water vapours (microbubbles). A high-voltage potential of ~4 kV was supplied between the gas input tube (1) and work liquid (3). The US transmitter worked at the frequency of 18 kHz with the power ~20 W. Different modes of the discharge operation with the “liquid” cathode were tested: I) with airflow and US; II) with airflow and without US; III) with US and without airflow; and IV) without airflow and US.

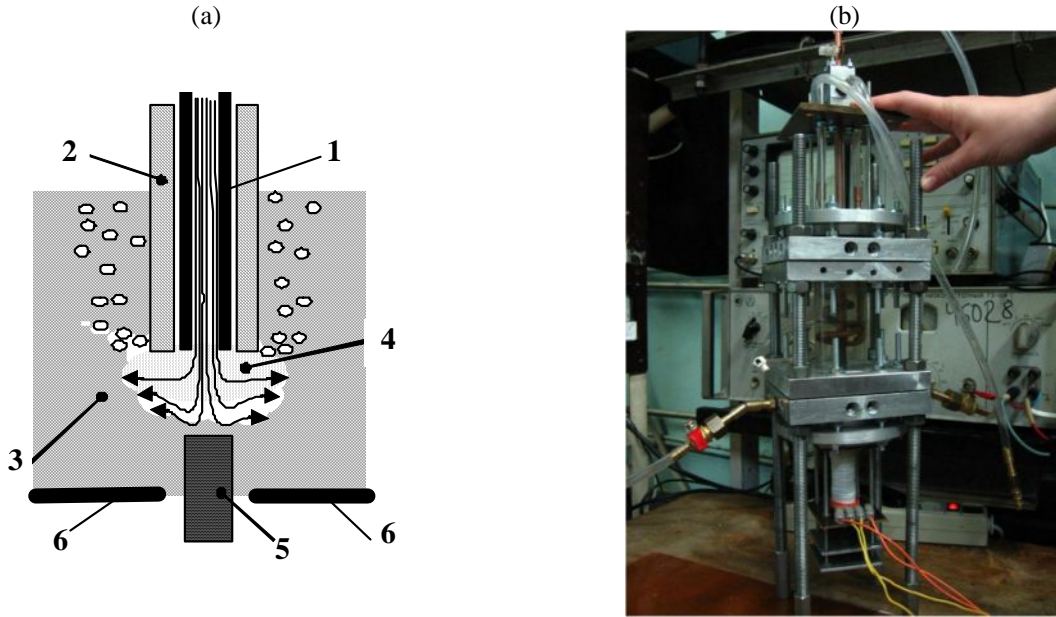


Fig. 3. DC DCGLW in the liquid with micropores (microbubbles) induced by US cavitations: (a) schematic of discharge with liquid cathode; (b) photo of the pulsed DGCLW reformer.

For safe utilization of the hydrogen-rich synthesis gas after the ethanol reforming in the PLS, a special gas-discharge system of plasma-assisted combustion based on dc discharge of BTA type was prepared (Fig. 4). Here, a jet of the air/fuel mixture of atmospheric pressure ran from the nozzle across two opposite rod electrodes and formed a bright crescent-shaped electric arc.

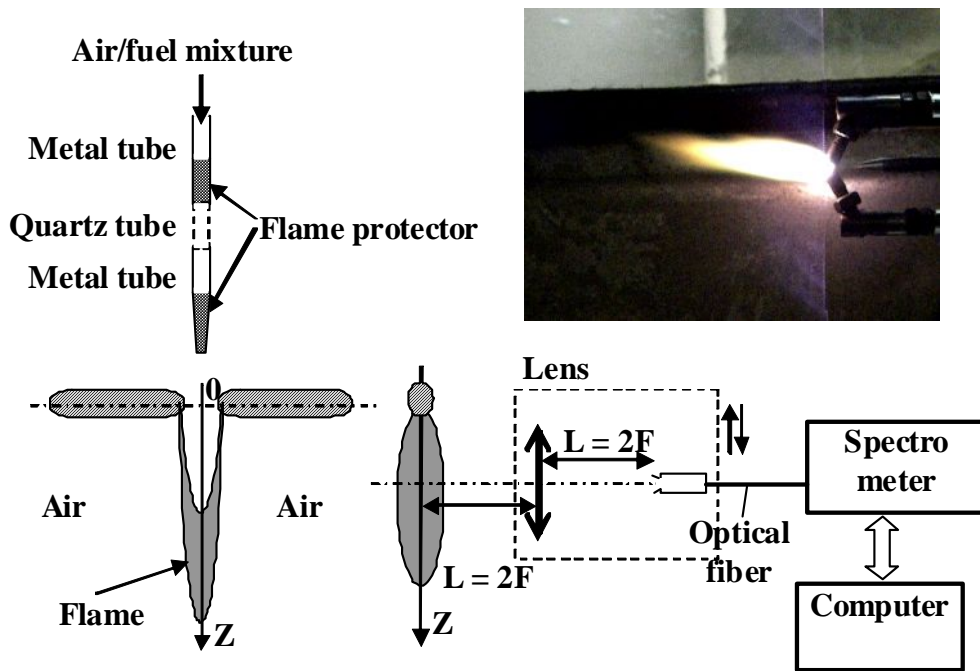


Fig. 4. CW discharge in the blowing transverse arc in air/fuel mixture: (a) schematic of discharge diagnostics; (b) photo of discharge plume.

We used the electrodes made from the copper rods with a diameter of 6 mm. A nominal gap between the electrodes was about 1 mm. The nozzle was axisymmetric with an inner diameter of 1 mm, made from stainless steel. It was maintained perpendicular to the electrode axis and was centred strictly between the electrodes. The air flow rate was usually $G = 110\text{cm}^3/\text{s}$. The BTA discharge was powered by the high-voltage DC power supply with the ballast resistance.

Besides the safety of laboratory experiments during the plasma fuel reforming, the BTA discharge system was used also in separate experiments on plasma-assisted combustion of premixed fuel/oxidant composition (synthesis gas after the plasma fuel reforming always is a premixed gas mixture containing oxygen). Then, this system was used also in calorimetric studies of fuel mixtures in the scheme of the plasma calorimeter (Fig. 5).

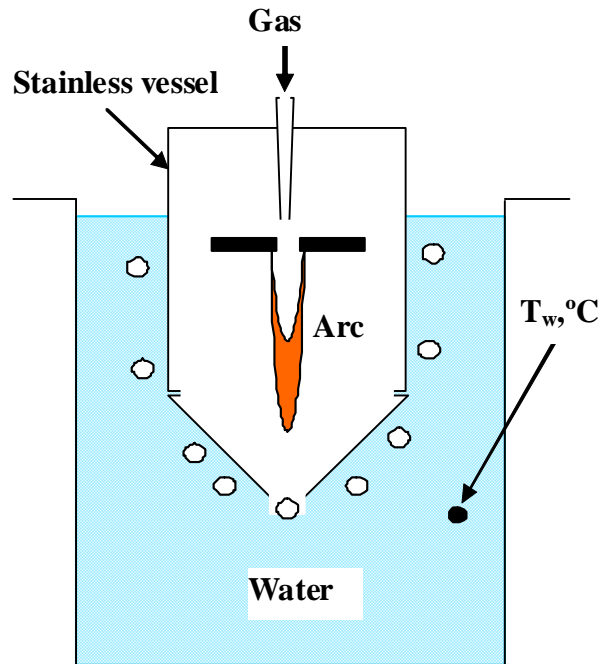


Fig. 5. Plasma calorimeter scheme.

In addition to direct plasma reforming, also pyrolysis of ethanol after initial plasma-assisted reforming was studied by using the unit shown in Fig. 6. The installation consists of two main parts: 1) plasma reactor, which treats ethanol-water mixture in the pulsed DGCLW, and 2) pyrolytic reactor, which treats ethanol-air vapors mixed with products generated by plasma reactor, where (1) is the Teflon insulator around the steel pins, (2) are steel pins through which voltage is applied, (3) are copper electrodes, conical bottom and top cylinder, (4) is a discharge plasma zone between electrodes, (5) is a vortex zone in the discharge, (6) is a bubbling zone in the liquid, (7) is the work liquid (solution of 96% pure ethanol and distilled water), (8) are mixing inlet and outlet chambers, (9) is the steel pyrolytic chamber; (10) are electric heaters, (11) is the cylindrical casing; (12) are thermocouples for temperature control, (13) is the glass vessel (0.5 l) for the output syngas collection.

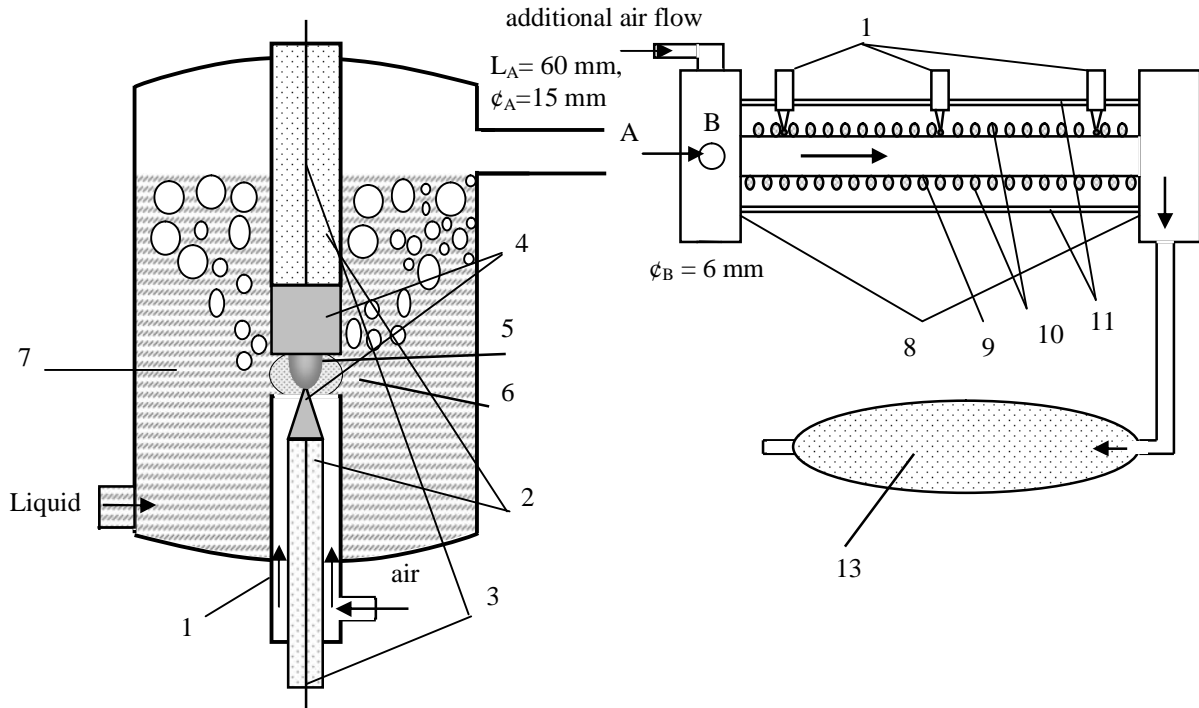


Fig. 6. Schematic of ethanol pyrolysis after plasma-assisted reforming of ethanol-water mixture in the pulsed DGCLW.

Diagnostic methods

Diagnostics of the DGCLW plasma was prepared by means of optical emission and absorption spectroscopy. The schematic of optical measurements is shown in Fig. 7.

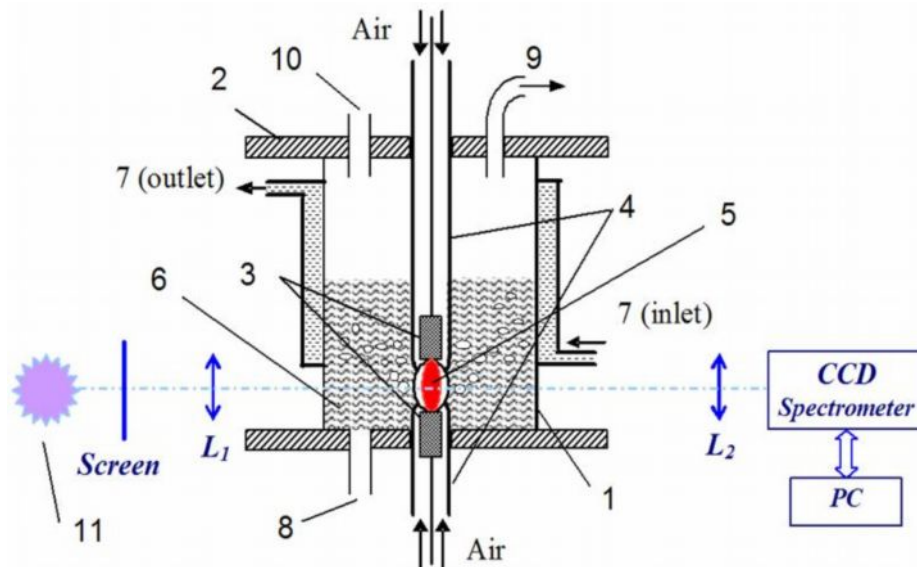


Fig. 7. Schematic of optical spectroscopy diagnostics of discharge plasma in the DGCLW.

Here, (1) is a quartz cylinder of the reactor, (2) are duralumin flanges, (3) are cooper electrodes, (4) are glass tubes for air input; (5) is a plasma column, (6) is the work liquid, (7) is a water cooling system, (8) is an input tube for work liquid, (9) is an output tube for gas products, (10) is a tube for the maintenance of constant pressure inside the reactor and communicating vessels, (11) is a spectral lamp source.

A high-speed CCD-based spectrometer “Plasmaspec” with a spectral resolution ~ 0.6 nm is used for the spectra registration in the range of wavelengths 200-1100 nm. The deuterium lamp is used as the etalon light source for measuring absorption spectra of plasma-treated liquids and making calibration for measuring the emission spectra of discharge plasma in the DGCLW.

According to spectral measurements, the emission spectra of the DGCLW plasma in the air-water system are multi-component (Fig. 8) and contain character atomic lines H (656.3; 486.1; 434.0 nm) and Cu (electrode material) (324.7; 327.4; 465.1; 510.5; 515.3; 521.8; 578.2 nm), molecular bands of the 2^+ -system of N_2 ($C^3\Pi_u-B^3\Pi_g$), UV system of OH ($A^2\Sigma-X^2\Pi$, (0-0): 306.4-308.9 nm), also NH band ($A^3\Pi^+-X^3\Sigma^-$) and NO γ -system ($A^2\Sigma^+-X^2\Pi$).

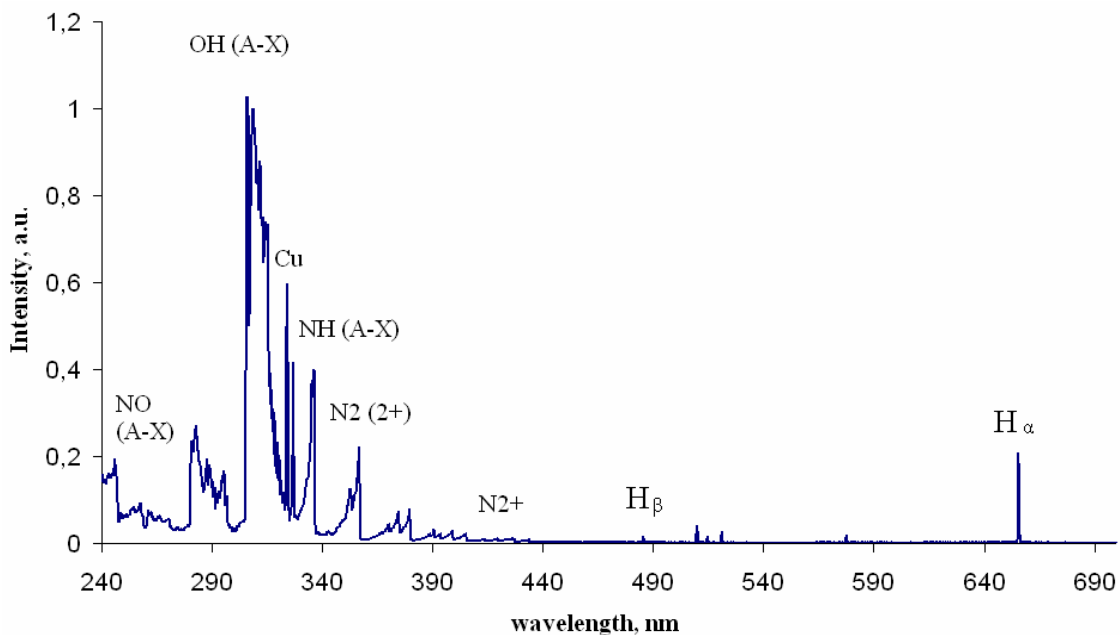


Fig. 8. Typical emission spectrum of air-water discharge plasma in the DCGLW.

The characteristic temperatures corresponding to excited states of atoms (electronic temperature T_e^*), and molecules (vibrational T_v^* and rotational T_r^* temperatures) in discharge plasma were determined by different methods. The electronic temperature T_e^* was determined by relative intensities of hydrogen emission lines H_α (656.3 nm) and H_β (486.1 nm) because these lines did no overlap with other spectral lines and bands. H_γ peak (434.0 nm) was not used because of its low intensity. Emission spectra of H lines were simulated by using a developed code Spec-Elements. This code allows calculations of absolute intensities of emission lines of elements (N, Ar, Cu, Fe, Ni, Co, Cr, etc) with using spectroscopic constants from the database of the Spectrum

Analyzer program [18] and taking into account the instrumental function of the spectrometer. To determine T_e^* both experimental and simulated spectra were normalized on the H_α peak. In this case the height of H_β peak will directly depend on the T_e^* value.

The electronic temperature T_e^* was determined also by relative intensities of emission of oxygen multiplet lines (777.2; 844.6; 926.6 nm). To increase the accuracy of T_e^* determining it is necessary to chose spectral lines corresponding to electronic transitions from the energy levels with the maximal energy discrepancies of upper excited states E_2 . Among OI lines observed in spectra the best pair is OI 777.2 nm ($E_2=10.74\text{eV}$) and OI 926.6 nm ($E_2=12.08\text{eV}$). Emission spectra of OI lines were simulated by using the SPECAIR program [19]. The dependence of the ratio of relative intensities of OI multiplet lines on the T_e^* values was plotted as a calibration curve. The spectral sensitivity of the used spectrometer was taken into account during the obtaining of corresponding intensities from experimental spectra.

To determine vibrational T_v^* and rotational T_r^* temperatures, an original technique with using the SPECAIR program was developed. Since the emission of the OH ($A^2\Sigma-X^2\Pi$) bands is very intensive and its spectral structure is well characterized, it is a good monitor of T_r^* in plasma [20]. It is a well-known method to use the P - and R - branches intensity ratio in the OH (0-0) band at wavelengths $\lambda=306.4\text{-}308.9$ nm for determination of T_r^* in plasma [21]. Because the peak of the P -branch is more self-absorbed than the peak of the R -branch, the P/R intensity ratio at given T_r^* becomes smaller as the optical thickness of plasma increases. A smaller P/R ratio would suggest T_r^* higher than its actual value. To avoid mistakes related with reabsorption it was proposed to use low intensive OH bands for determining T_r^* . A technique based on the SPECAIR simulation of the OH (1-0) and (2-1) bands, which are free from reabsorption, was suggested.

First of all, it was necessary to know spectral regions of the OH emission without overlapping with other spectral lines and bands. For that, emission spectra of main components of air-water plasma were simulated separately by the SPECAIR. Then, it was important to find out what spectral regions are sensitive for T_r^* and T_v^* temperatures. For that, the SPECAIR simulation of the OH emission in the spectral range 275-300 nm for different T_v^* at fixed T_r^* and for different T_r^* at fixed T_v^* was made. The main results are presented in Fig. 9.

It was shown that a tilt angle of the OH (1-0) band at $\lambda=283.1$ nm “red shading” (in the spectral interval 283.1-286.9 nm) depends just on T_r^* and does not depend on T_v^* . Therefore, at the first stage the temperature grid of T_r^* values with the constant step, which corresponds to the accuracy of measurements, was calculated under the fixed arbitrary T_v^* value. It was proposed to normalize the OH band (1-0) at $\lambda=283.1$ nm. Then, characteristic relative intensities (heights) **A**, **B** and **C** near the characteristic maxima and minima at the fixed wavelengths were chosen. The counting of its heights was made from the initial background **D** at $\lambda=273.8$ nm. It depends neither on T_v^* nor T_r^* in the wide temperature range that is why it is zero as shown in Fig. 9. In the case of the overlapping, for example, with the NO emission, all relative intensities of the OH emission should be measured from its background at $\lambda=273.8$ nm.

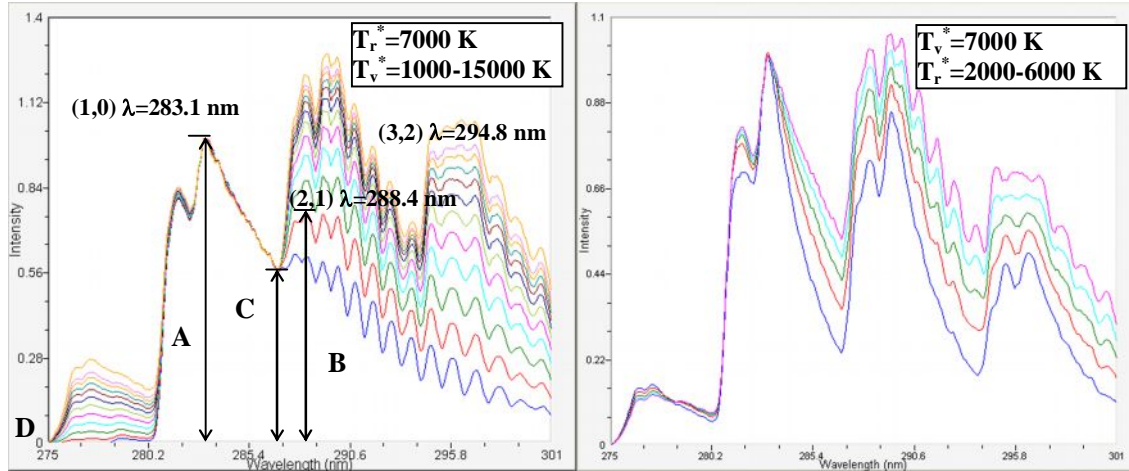


Fig. 9. SPECAIR simulation of OH (A-X) emission bands in the range of wavelengths 275-300 nm at different temperatures T_r^* and T_v^* . **A** is the intensity of the band (1-0) at 283.1 nm; **B** is the intensity of the band (2-1) at 288.4 nm; **C** is the intensity at 286.9 nm.

To simplify the determining of T_r^* , the calibration curve (i.e. relative intensity C/A as a function of T_r^*) was plotted (Fig. 10a). The next stage was to fix the T_r^* value that was found at the previous step and to calculate the temperature grid of T_v^* to plot the corresponding calibration curves $(B-C)/A$ as relative intensities of (2-1) to (1-0) bands (Fig. 10b).

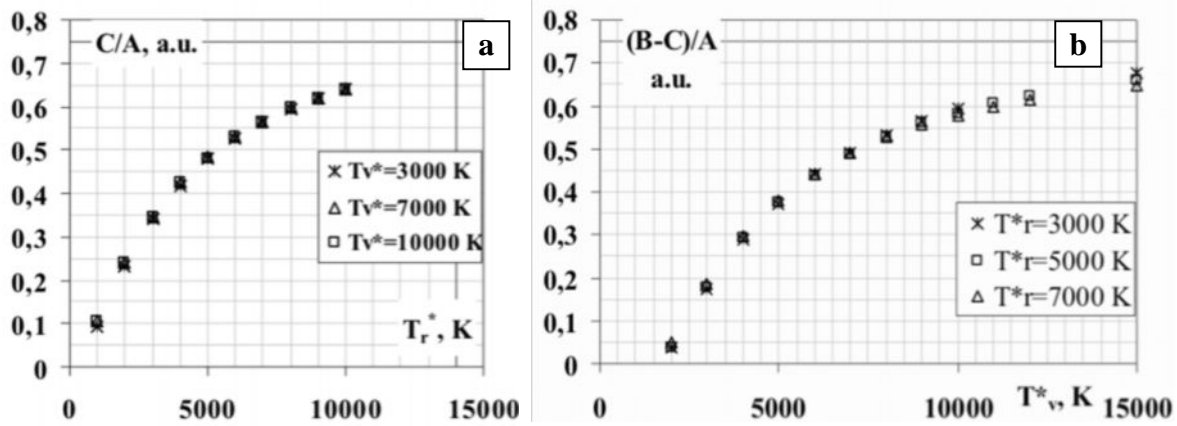


Fig. 10. Calibration curves for determining of temperatures T_r^* and T_v^* by OH (A-X) bands obtained by using the SPECAIR with the instrumental function of the used spectrometer FWHM= 0.6 nm: (a) graph for T_r^* ; (b) graph for T_v^* .

From Fig. 10a we see that the ratio C/A does not depend on T_v^* (all curves coincide), so we can use it for determination of T_r^* . By analogy from Fig. 10b we see that the ratio $(B-C)/A$ does not depend on T_r^* , so we can use it for estimation of T_v^* within the investigated temperature range. Since we obtained the calibration curves, which are functions only one excitation temperature, T_v^* or T_r^* , it is inessential in what sequence temperatures were determined in that case.

In air plasma that contains nitrogen, a good tool for diagnostics is the emission of molecular bands of the 2^+ -system of N_2 ($C^3\Pi_u-B^3\Pi_g$). It includes the bands (0-0) at 337.1 nm, (0-1) at 357.7 nm, (0-2) at 380.5 nm, (0-3) at 405.9 nm, (1-0) at 315.9 nm, (1-2) at 353.7 nm, (1-3) at 375.5 nm, (1-4) at 399.8 nm, (2-0) at 297.7 nm, etc. To find spectral regions without overlapping with other spectral lines and bands, emission spectra of main components in air-water vapor system at atmospheric pressure were simulated separately by the SPECAIR. Results are shown in Fig. 11.

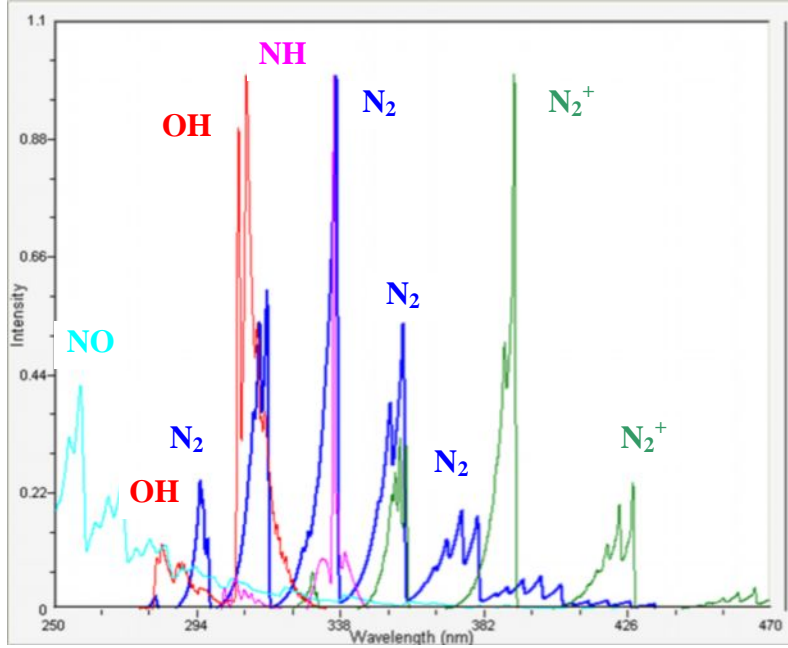


Fig. 11. SPECAIR simulation of N_2 (C-B), N_2^+ (B-X), NH (A-X), OH (A-X), NO (A-X) emissions at $T_e^*=T_v^*=T_r^*=4000$ K. Each spectrum is normalized at its maximum.

From Fig. 11 one can see two spectral regions, which are almost free from the overlapping for the N_2 (C-B) emission. Since N_2 (C-B) bands (0-3) and (1-4) are low intensive, it is better to use (0-2) and (1-3) bands in the spectral range 360-380 nm. When the N_2^+ (B-X) intensity is not very high (nearly 3 times less) in comparison with the N_2 (C-B), its “tail” (violet degradation) does not influence too much on the intensity of (0-2) and (1-3) bands. It was proposed to use the width of the N_2 (C-B) band (0-2) at the 20% and 40% height of the peak intensity as a function of temperatures T_r^* in the case when it is impossible to compare the experimental spectrum with the SPECAIR simulation. The results are presented in Fig. 12.

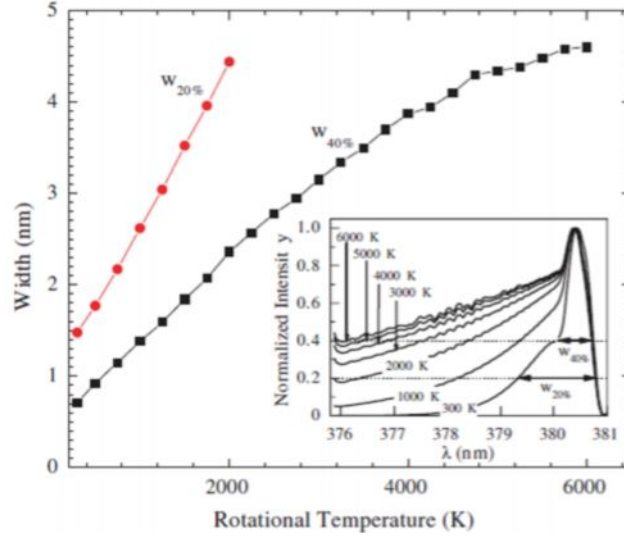


Fig. 12. Spectral widths of the N₂ (C-B) band (0-2) at 20% and 40% of the peak's height calculated by the SPECAIR assuming the trapezoidal slit function of the base 0.66 nm and the top of 0.22 nm at different temperatures T_r^* , normalized to the peak at 380.4 nm.

Since N₂ bands (0-2) and (1-3) are overlapping, it is difficult to separate them. It was suggested to take relative intensities (heights) near the characteristic maxima and minima at the fixed wavelengths for plotting of calibration curves for N₂ (C-B) bands in the same way as for OH (A-X) bands. The spectral regions, which are sensitive for T_r^* and T_v^* temperatures, were determined by using the SPECAIR simulation of the N₂ (C-B) emission in the spectral range 360-380 nm for different T_v^* at fixed T_r^* and for different T_r^* at fixed T_v^* . The results are presented in Fig. 13.

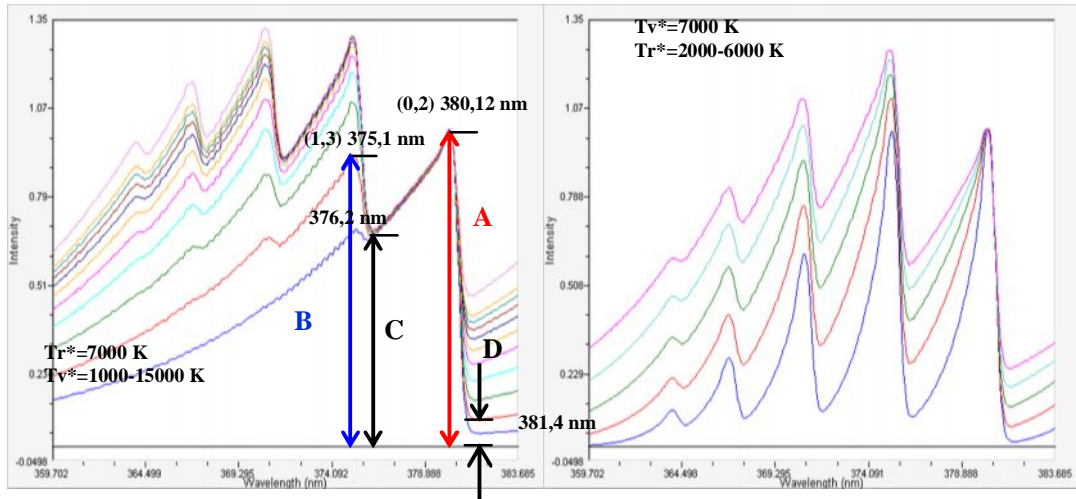


Fig. 13. SPECAIR simulation of N₂ (C-B) emission bands in the range 360-380 nm at different temperatures T_r^* and T_v^* . **A** is the intensity of the band (0-2) at 380.1 nm; **B** is the intensity of the band (1-3) at 375.1 nm; **C** is the intensity at 376.2 nm; **D** is the intensity at 381.4 nm.

The corresponding relative intensities at the fixed wavelengths and the calibration curves C/A and $(B-C)/(A-D)$ for determining of T_r^* and T_v^* are plotted in Fig. 14. Since the head of the N_2 (C-B) band (0-2) overlaps with the tails of other bands at the right side, it is necessary to take into account the height of the **D** (intensity at 381.4 nm) at the plotting of calibration curves (Fig. 15). As is seen, the calibration curves for determining T_r^* do not coincide for different T_v^* because the height of the **D** depends on both T_r^* and T_v^* . That is why it is necessary to determine first T_v^* by using the curve $(B-C)/(A-D)$ (Fig. 14 a) and then determine T_r^* by using the set of curves $(C-D)/(A-D)$ (Fig. 15).

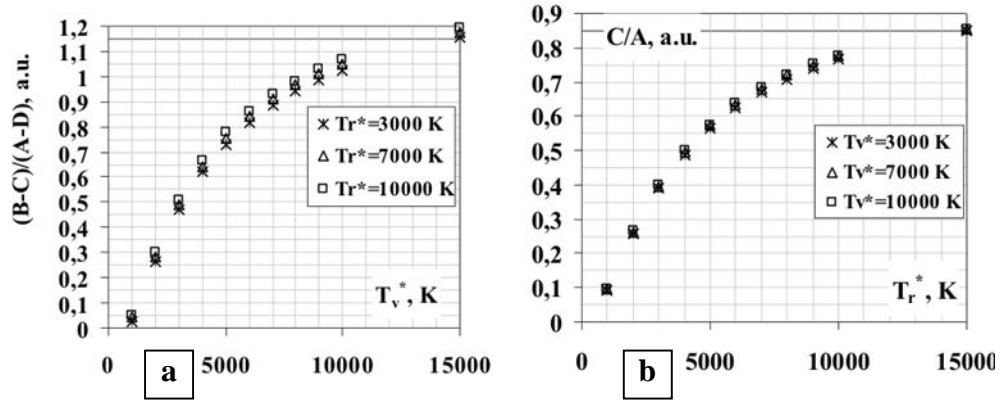


Fig. 14. Calibration curves for determining of temperatures T_r^* and T_v^* by N_2 (C-B) bands obtained by using the SPECAIR with the instrumental function of the used spectrometer FWHM=0.6 nm: (a) graph for T_r^* ; (b) graph for T_v^* .

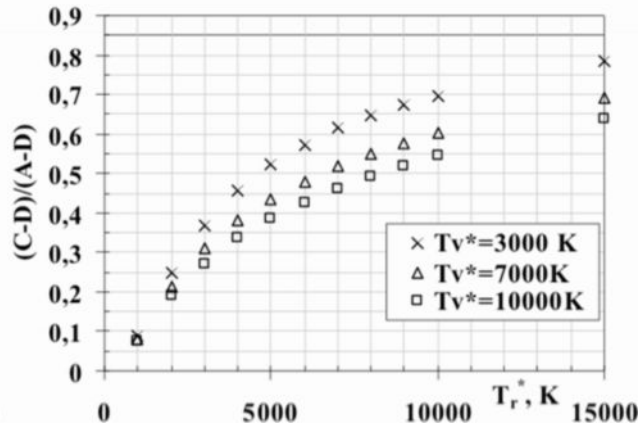


Fig. 15. Calibration curves for determining of temperature T_r^* by N_2 (C-B) bands obtained by using the SPECAIR with the instrumental function of the used spectrometer FWHM=0.6 nm.

The similar spectral simulations were made for the C_2 Swan system ($d^3\Pi_g-a^3\Pi_u$): band (0-0) at 516.5 nm and for the CN UV system ($B^2\Sigma^+-X^2\Sigma^+$): band (0-0) at 388.3 nm by using the SPECAIR in the same way as for the N_2 (C-B) emission. The spectral intervals sensitive for T_r^* and T_v^* temperatures were determined, dependences of relative intensities near the characteristic maxima and minima at the fixed wavelengths were obtained (Fig. 16) and the calibration curves to simplify spectra processing were plotted (Fig. 17).

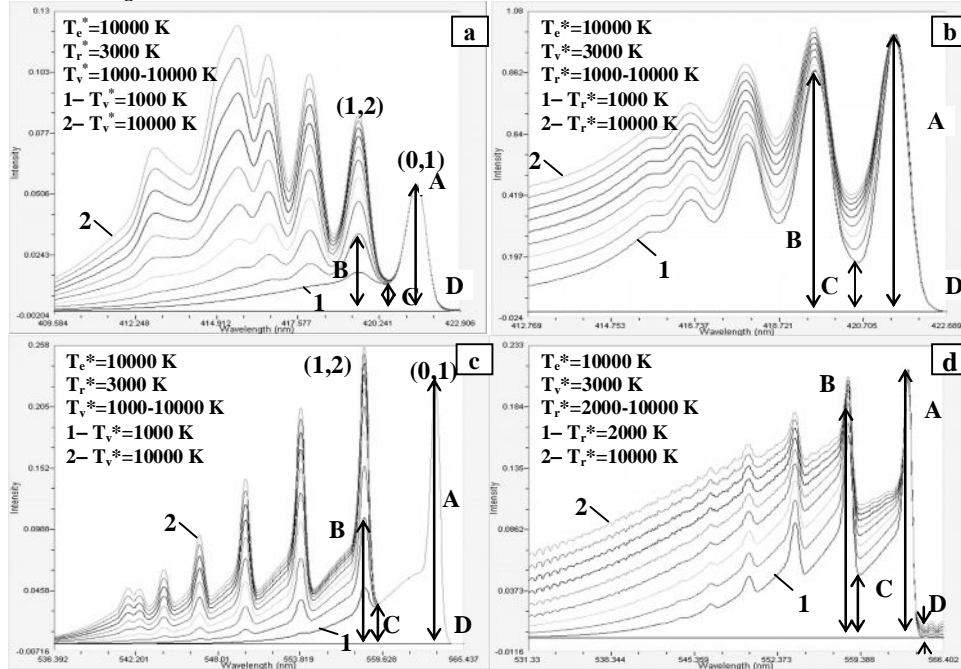


Fig. 16. Graphs (a), (b) are spectral simulation of the CN (B-X) emission in the range 410-422 nm: **A** and **B** are intensities of the bands (0-1) at 421.45 nm and (1-2) at 419.56 nm; **C** and **D** are intensities at 420.5 and 422.6 nm, respectively. Graphs (c), (d) are spectral simulation of the C₂ (d-a) emission in the range 530-566 nm: **A** and **B** are intensities of the bands (0-1) at 563.42 nm and (1-2) nm at 558.3 nm; **C** and **D** are intensities at 559.37 and 564.54 nm, respectively.

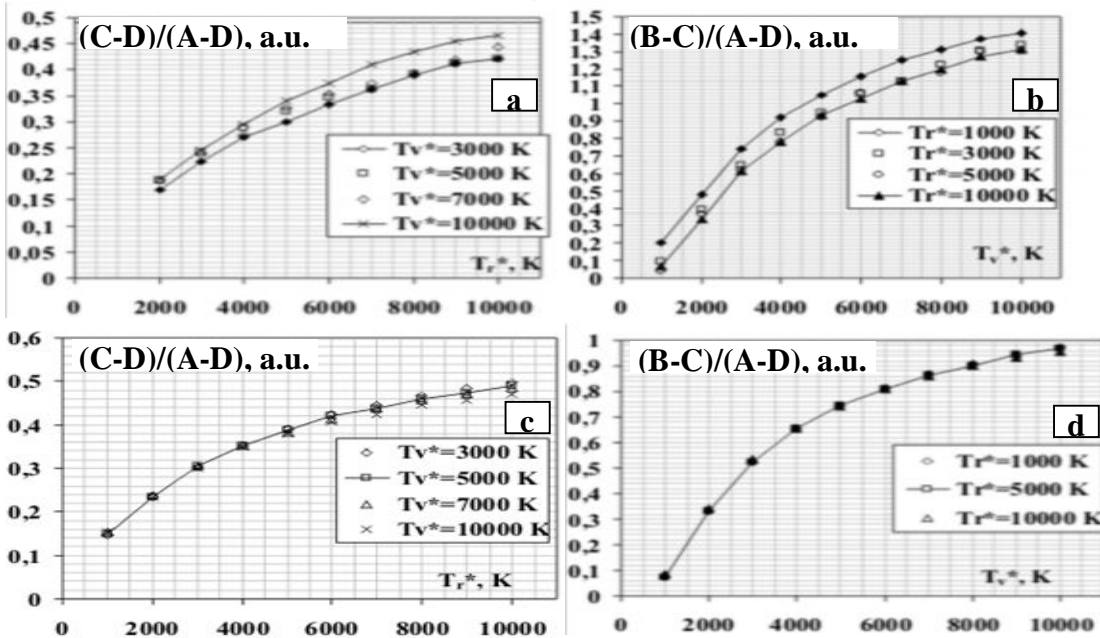


Fig. 17. Calibration curves for determining of temperatures T_v^* and T_r^* by CN (B-X) bands (graphs a, b) and by C₂ (d-a) bands (graphs c, d) obtained by using the SPECAIR with the Gaussian instrumental function of the used spectrometer FWHM= 0.6 nm: (a), (c) graphs for T_r^* ; (b), (d) graphs for T_v^* , respectively.

The developed methods were applied for OES diagnostics of discharge plasma parameters in different regimes of the DGCLW operation in ethanol-water mixtures as well as for diagnostics of the BTA discharge working in ethanol-air mixture.

Emission spectra were measured by the CCD spectrometer “Plasmaspec” as described before. The absolute intensities of calculated spectrum $I_{cal}(A_i)$ by using the SPECAIR at the fixed wavelengths (where the corresponding experimental signals $I_{exp}(A_i)$ were estimated) were determined. Then, the ratio of concentrations of radiating species A and B was evaluated by following formula:

$$\frac{[A_1]}{[A_2]} = \frac{I_{exp}(A_1) \cdot I_{cal}(A_2)}{I_{exp}(A_2) \cdot I_{cal}(A_1)}, \quad (1)$$

This makes possible to determine the relative concentration of each component in the investigated discharge plasma:

$$[A_i]^* = \frac{[A_i]}{\sum_i [A_i]} \quad (2)$$

The typical emission spectrum of the BTA discharge plasma in ethanol/air mixture is shown in Fig. 18. Here, among molecular bands, we recognised the NO γ -system ($A^2\Sigma^+ - X^2\Pi$: (0-0) 226.9 nm, (0-1) 236.3 nm, (0-2) 247.1 nm, etc); OH UV system ($A^2\Sigma - X^2\Pi$: (0-0) 306.4-308.9 nm); and N_2 2^+ system ($C^3\Pi_u - B^3\Pi_g$: (0-0) 337.1, (0-1) 357.7, (0-2) 380.5, (1-0) 316.0 nm, etc). Among atomic lines, we recognized the HI Balmer lines (656.3, 486.1 nm), OI lines (777.3, 844.6, 926.0 nm), and NI lines (746.8, 818.8, 868.3 nm). There are a lot of Cu lines (due to evaporation of copper electrodes) but we used CuI lines 465.1, 510.5, 515.3, 521.8, and 578.2 nm only because the strongest CuI lines 324.7 and 327.4 nm are resonant and can be self-absorbed.

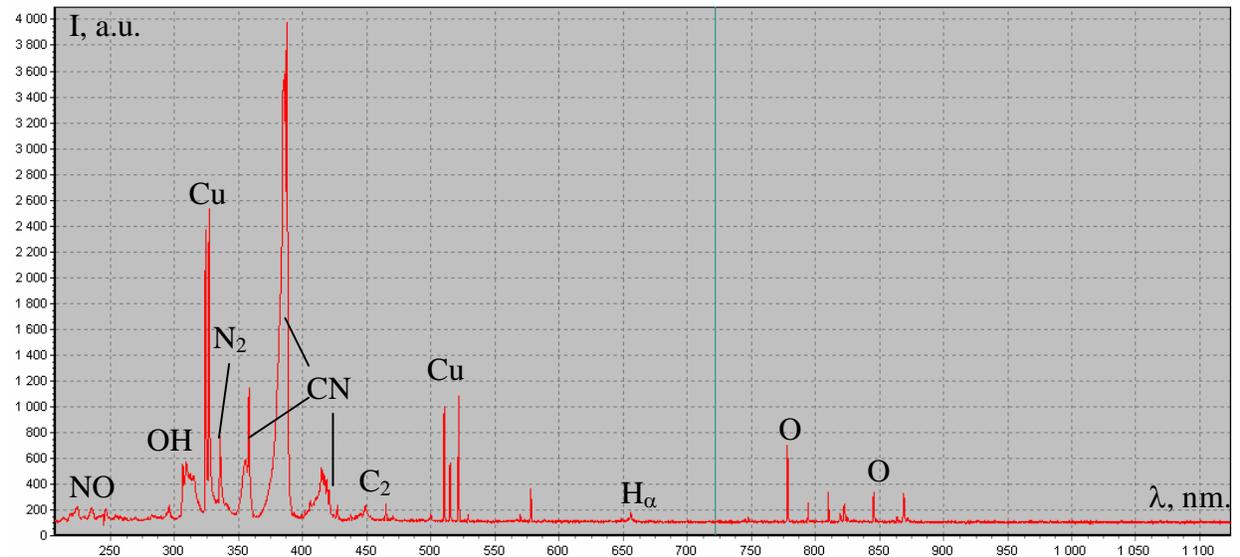


Fig. 18. Typical emission spectrum of the BTA discharge in ethanol/air mixture.
 $I_d = 400$ mA, $G = 75$ cm³/s

Diagnostics by mass-spectrometry using a monopole mass-spectrometer MX 7301 and by gas-phase chromatography using a gas chromatograph 6890 N Agilent with the calibrated thermal conductivity detectors were prepared for the analysis of component content of the output gas products after the processing in the plasma-chemical reactor.

The typical mass spectrum of output gas products registered after the processing of ethanol-water mixture is shown in Fig. 19. We have recognized the character components related to the mass ratios $M/e = 2$ (H_2^+), 12 (C^+), 14 (N^+), 16 (O^+ , CH_4^+), 18 (H_2O^+), 28 (CO^+ , N_2^+), and 32 (O_2^+).

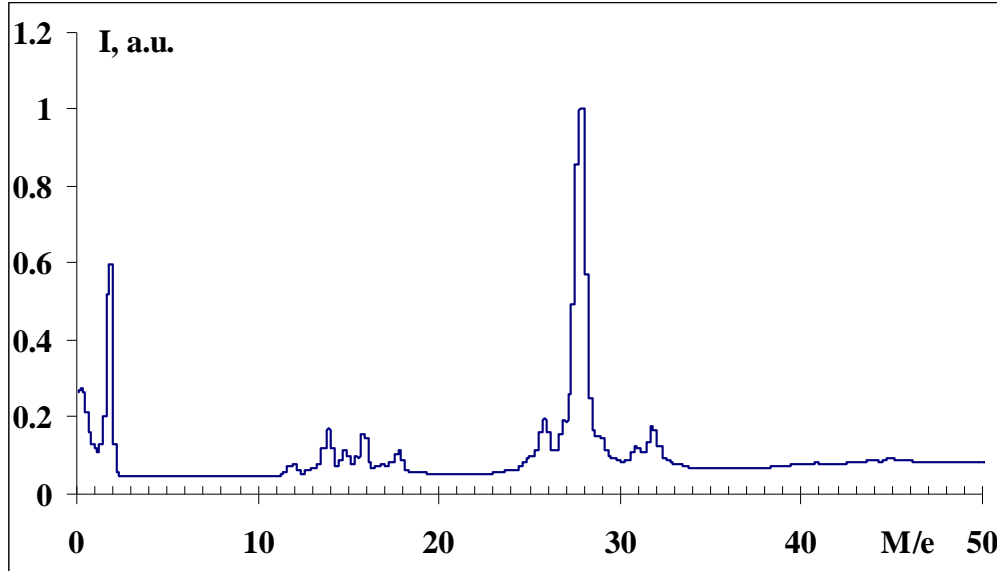


Fig. 19. Typical mass-spectrum of output gas products after the plasma reforming of ethanol-water mixture in the PLS with the DGCLW with the liquid cathode. $I_d=300$ mA, $G= 55$ cm³/s

Numerical models

The physical model of DGCLW-PLS was based on the next assumptions:

- electric power introduced in the discharge is immediately averaged in the discharge volume;
- internal electric field in the discharge does not vary in space and time;
- during the pass of air through the discharge into the reactor volume its content is totally refreshed and its flow rate in the reactor volume is the same as in the discharge gap.

The mathematical modeling of DGCLW-PLS was developed with the next features:

- calculation of the electron energy distribution function on the base of solution of the Boltzmann equation in two-term approximation [22];
- hydrodynamic modeling in quasi-1D fluid volume averaged approximation [23];
- kinetic modeling by solution of the system of chemical kinetic equations for kinetically valuable components of air-ethanol-water plasma system [24].

The kinetic mechanism includes 59 components (C_2H_5OH , N_2 , O_2 , H_2O , H_2 , CO , etc), 76 electron-molecular processes and 364 chemical reactions with a set of corresponding cross sections and rate constants compiled according to update NIST kinetic databases [25].

As a case study, the comparative analysis of the developed method of simulation of kinetic processes in the plasma-liquid system in the electrical discharge in the gas channel with liquid wall and other known methods of calculations of plasma kinetics in micro-discharges was conducted. It was shown that the averaging of the energy that deposited into the discharge in the whole gas channel volume is the principal feature of the developed method.

Modeling of dusty plasmas with liquid microparticles

Complex (dusty) plasmas are gas plasmas consisting of electrons, ions, and neutral atoms that additionally contain microscopic particles with sizes ranging from 10 nm to 10 μm . These microparticles may be solid or liquid. It is well-known [26] that many features of these states are very similar. From this point of view will be useful produce a review of generalities of both types of microparticles and give a special account of distinctive features of liquid substances. Essential differences of liquid particle from solid one mostly connected with special features of liquid surface. It is clear that addition of electric charge makes new peculiarities in this situation.

The main parameters of liquid drop are:

- 1) geometrical – what type of approximation is selected: ball-shaped (main factor is its radius) or spheroid (main factor is its eccentricity);
- 2) physical – mass/volume density; dielectric permittivity; surface tension coefficient; viscosity; specific conductivity; evaporation and coagulation;
- 3) chemical – composition; existence of surface-active substance (SAS).

The theoretical model should describe basic phenomena in dusty plasma. They are:

- I. Elementary processes in dusty plasma;
- II. Dynamical processes in dusty plasma;
- III. Waves and instabilities in dusty plasmas.

We can provide some quality conclusions:

1. The droplet surface is unstable, because thermal capillary waves are disturbed.
2. The maximal surface charge (Q_{max}) exists.
3. This charge (Q_{max}) is the reason of drop decay. The method of solving this problem arise from Bohr – Frenkel theory of nuclear decay.
4. The decay path is a function of viscosity (γ) and dielectric permittivity (ϵ) = $f(\epsilon, \gamma)$. If liquid in drop has a conductivity and its viscosity is small, the drop will be disintegrated on some hundreds little droplets with radius $a_i \ll R$. If liquid in drop is dielectric, the drop has 2-particle decay. Their full charge is equal to initial Q and their radius $a_i \leq R$.
5. Changes in chemical composition or SAS additions make the surface charge variability.
6. Interaction of charged drop with laminar air flow is resulted decay criterion lower.
7. Linear vibration of charged drop surface can produce the electromagnetic radiation.
8. Surface of uncharged drop (incompressible) can produce the acoustic wave in definite frequency range. Surface charging will intensify this effect. It can be used for diagnostics of liquid dusty particles in plasma of the DGCLW.

RESULTS AND DISCUSSION

The applicability of the developed methods for diagnostics of the discharge plasma parameters was tested in the DGCLW in different modes of operation: with two solid electrodes or with one liquid electrode of different polarity, i.e., liquid anode or liquid cathode.

Typical operating parameters in nominal regime were following: discharge current $I_d = 200$ mA, voltage $U = 1.6$ kV, airflow rate $G = 55$ cm³/s. Emission spectra of investigated plasma were registered by the CCD spectrometer “Plasmaspec” in the range of wavelengths $\lambda = 200$ -1100 nm.

For estimation of electronic excitation temperatures T_e^* in plasma, the relative intensities of atomic emission lines of Cu ($\lambda = 465.1; 510.5; 515.3; 521.8; 578.2$ nm) and H ($\lambda = 486.1, 656.6$ nm) were analyzed. As a result, a set of characteristic electronic temperatures $T_e^*(H) = 4300$ K and $T_e^*(Cu) = 7200$ K was obtained for the investigated regime of the discharge operation.

For estimation of vibrational and rotational excitation temperatures T_v^* and T_r^* in plasma, the relative intensities of molecular emissions of the OH (A-X) bands (1-0) at 283.1 nm and (2-1) at 288.4 nm and the N₂ (C-B) bands (0-2) at 380.1 nm and (1-3) at 375.1 nm were analyzed on the base of the SPECAIR simulation. Results of the fitting of experimental and simulation spectra in the selected spectral intervals are shown in Fig. 20.

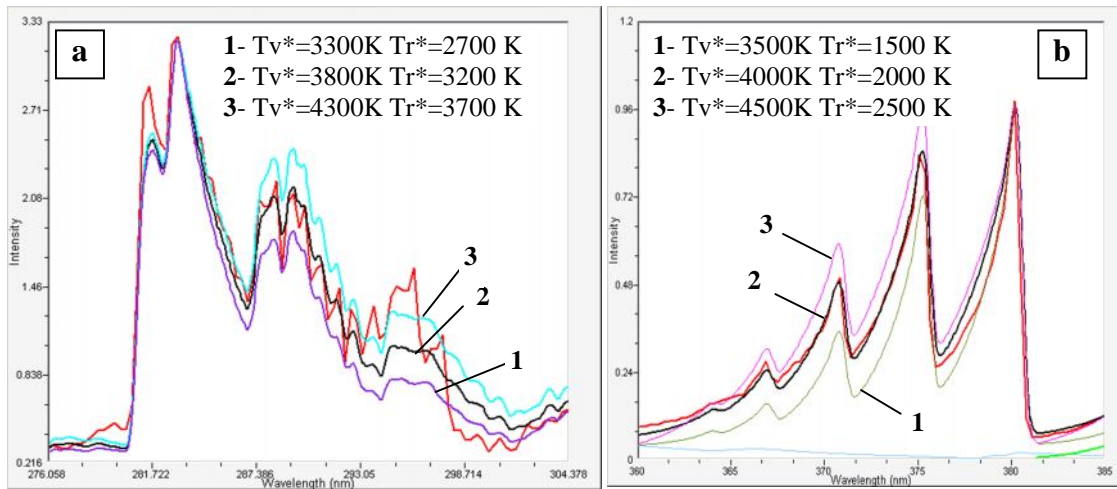


Fig. 20. SPECAIR simulation (curves 1, 2, 3) and experimental (red curve) spectra of the DGCLW in water: (a) OH (A-X) bands at 275-304 nm; (b) N₂ (C-B) bands at 360-385 nm.

The best fit in Fig. 20 was found for the following set of temperatures: $T_v^*(OH) = 3800$ K, $T_r^*(OH) = 3200$ K, $T_v^*(N_2) = 4000$ K, $T_r^*(N_2) = 2000$ K. The discrepancy between measured and calculated spectra in Fig. 20a in contrast to Fig. 20b can be explained by the fact that the simulation of the OH (A-X) emission was made without taking into account the N₂ (C-B) emission that occurs in the same spectral region. The comparison of measured and calculated spectra in the more wide spectral ranges is presented in Fig. 21. One can see it looks good.

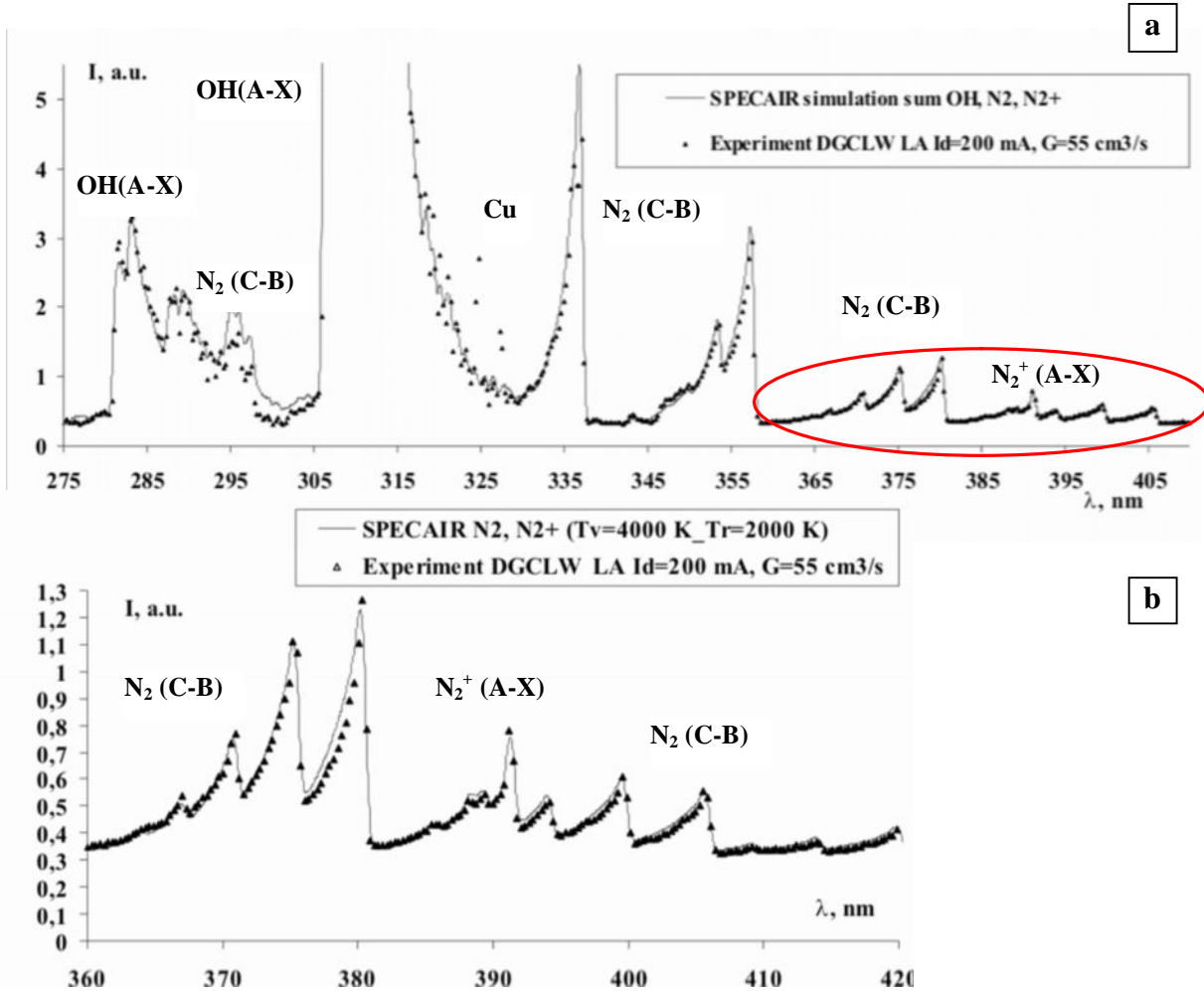


Fig. 21. SPECAIR simulation and experimental spectra of the DGCLW in water: (a) emission in the range 275-405 nm; (b) magnified spectral range 360-420 nm in the red oval. Characteristic temperatures: T_v^* (OH)=3800 K, T_r^* (OH)=3200 K, T_v^* (N₂, N₂⁺)=4000 K, T_r^* (N₂, N₂⁺)=2000 K.

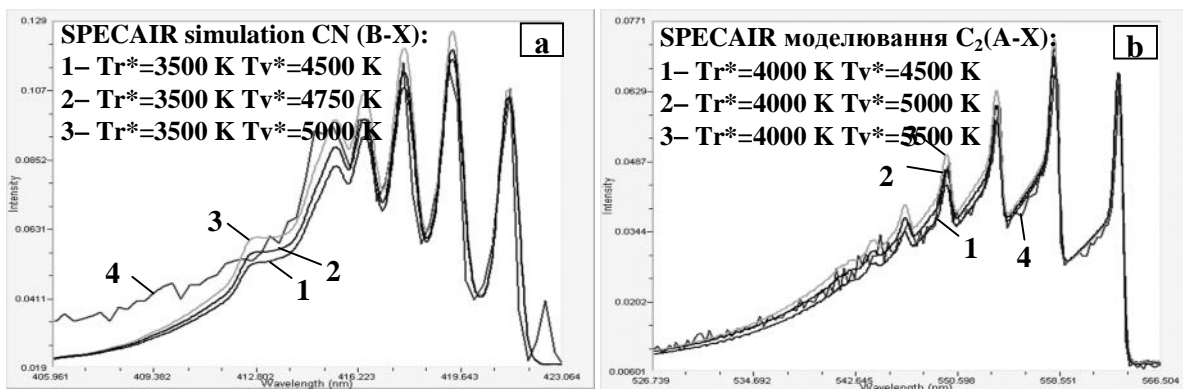


Fig. 22. SPECAIR simulation (curves 1, 2, 3) and experimental (curve 4) spectra of the DGCLW in ethanol: (a) CN (B-X) bands at 406-423 nm; (b) C₂ (d-a) bands at 528-565 nm.

The same technique was applied also for diagnostics of the BTA discharge in air and ethanol/air mixtures of different ethanol content (1/33–1/8 mol). The emission spectra were registered in the different cross-sections along the plasma plume. The distributions of the character excitation temperatures T_e^* , T_v^* and T_r^* for Cu, O atoms and N_2 molecules were determined as shown in Fig. 23a; distributions of the relative mole fractions of radiating species N_2 , OH, NO and NH in plasma along the flow are shown in Fig. 23b. Here, z is the direction of the flow: the point $z=0$ corresponds to the axe of the electrodes. From Fig. 23 one can see that the plasma plume in air is non-isothermal. As for electronic temperatures for Cu atoms in comparison with O atoms in the investigated plasma, $T_e^*(Cu)$ exceeds $T_e^*(O)$ in 1.5 times.

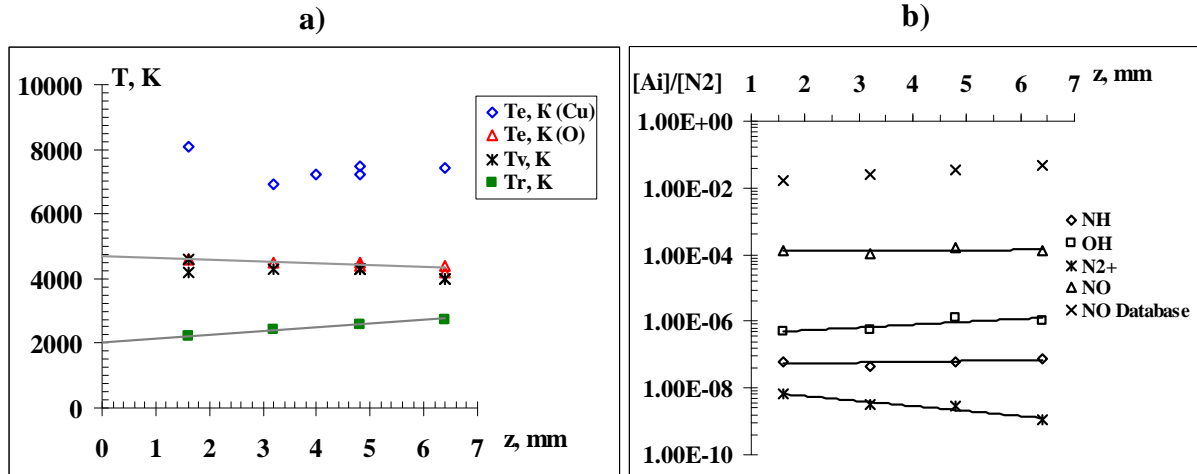


Fig. 23. Distribution (a) character temperatures and (b) relative mole fractions of species along the flow in the BTA working in air. The current $I_d=480$ mA; airflow rate $G=75$ cm³/s.

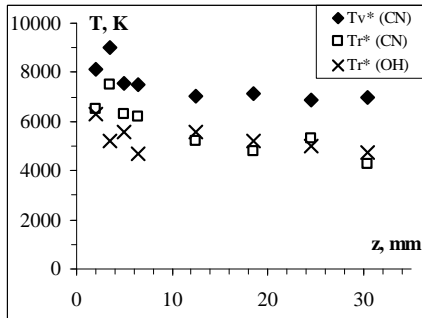


Fig. 24. T_v^* , T_r^* along the flow for air/ethanol mix (8/1 mole).

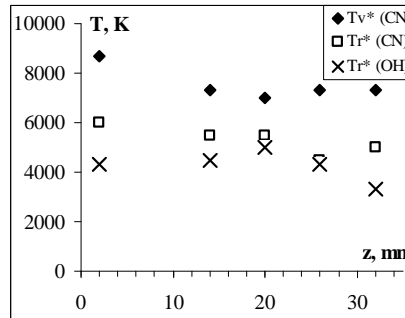


Fig. 25. T_v^* , T_r^* along the flow for air/ethanol mix (15/1 mole).

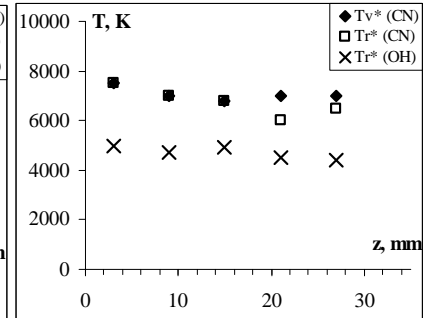


Fig. 26. T_v^* , T_r^* along the flow for air/ethanol mix (33/1 mole).

The distributions of temperatures T_v^* and T_r^* determined from the OH (A-X) and CN (B-X) emissions along the plasma plume at different air/ethanol ratios are shown in Figs. 24-26. One can see that these dependencies greatly differ from the results obtained for the BTA in air. The T_v^* , T_r^* are highest near the electrodes then they do not vary very much along the flow. The high level of $T_r^*(CN)$ can be explained by the presence of combustion processes in air/fuel mixture. The discrepancy of $T_r^*(OH)$ determined by the R/P peaks ratio from the OH (A-X) band (0-0) can be explained by the inaccuracy of estimations. Since the peak P of the OH band overlaps with N_2 (C-B) bands, its intensity is overstated and the obtained T_r^* is understated.

Applying the absorption spectrophotometry, we measured the absorption spectra of work liquids after the plasma treatment in the DGCLW-PLS reactor with US and without US cavitations. According to measurements (Fig. 27), the absorption spectra of the treated liquid consist of UV absorption bands of ions of nitrous acid HNO_2 . Its spectral distribution does not change very much with and without US treatment, but the intensity of the absorption band at 350 nm permanently grows with the exposure time (Fig. 27.a). It means that the concentration of the HNO_2 products in the treated liquid grows proportionally to the time of the plasma treatment, and this process proceeds more intensively under the influence of the US cavitations (Fig. 27.b).

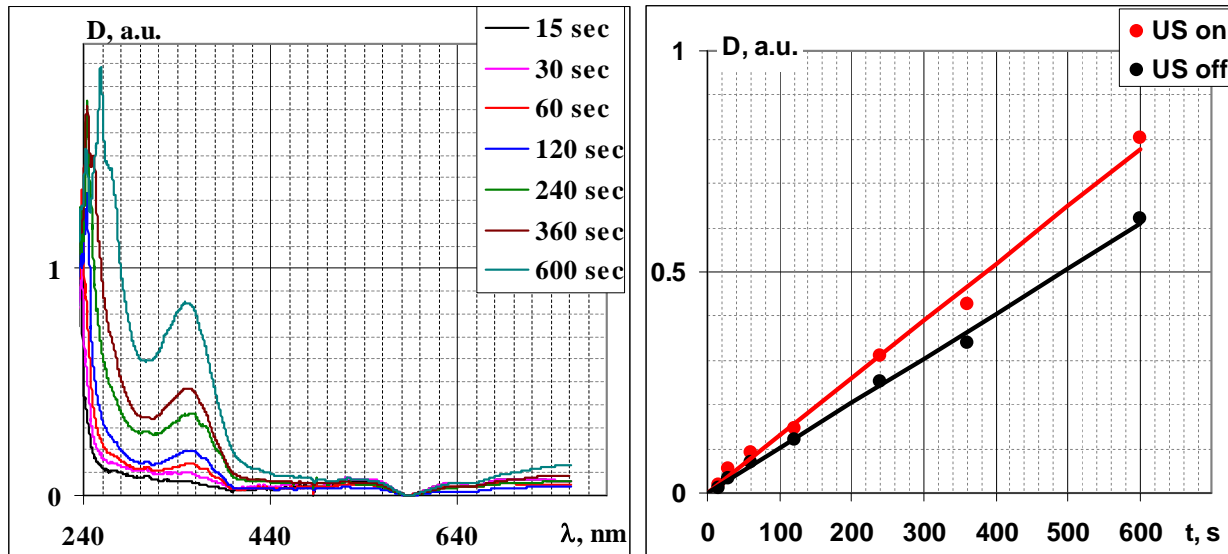


Fig. 27. Absorption spectra (left) of water solution after the plasma treatment in the DGCLW for different processing times (curves 1-7 are from 15 to 600 s) and dependences (right) of UV absorption at 380 nm on the exposure time in the discharge with US (grey curve) and without US cavitations (black curve).

Analyzing the emission spectra in plasma of the pulsed DGCLW working in different modes with and without US field, the dependences of relative intensities of molecular OH (A-X) and N_2 (C-B) bands and atomic H_α , H_β lines were obtained. Also, using the ratio of H_α and H_β lines, the temperature of the population of H electronic states $T_e^*(\text{H})$ was estimated.

It was found that the US field differently affects the behavior of various components of plasma emission in the DGCLW. From Fig. 28 one can see that without US field the relative intensity of OH (A-X) emission nonmonotonically increases with increasing exposure time, but it quickly reduces under the US cavitations. Relative intensity of N_2 (C-B) emission is almost independent on exposure time with and without US field.

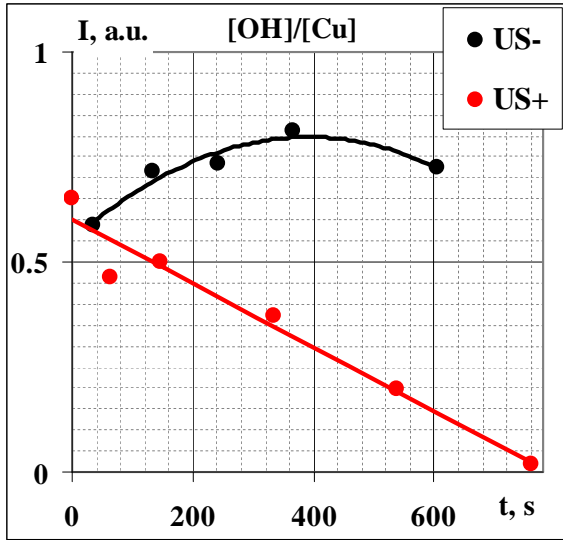


Fig. 28. Relative intensity of the OH emission in plasma of the DGCLW working in pure water vs. exposure time. Grey curve is the US on, black curve is the US off.

Relative intensity of H_{α} emission linearly increases with increasing exposure time in both modes with and without US; however, the US field reduces the rate of this growth for half time. Despite the growth of the relative H_{α} emission intensity, the electronic temperatures $T_e^*(H)$ are virtually the same, i.e. the US field has no visual effect on the behavior of T_e^* .

It is important to note that all components of emission spectra observed have lower relative emission intensities in the presence of the US field. This can be explained that the US at 17 kHz may be easily transmitted in air. Moreover, the features of the plasma-liquid surface interaction at the boundary between the phases can favor to the penetration of the US field into the gas phase. Then, the US cavitations in plasma can increase the probability of the quenching of excited states of atoms due to enhanced collisions.

As a result, total intensity of radiation in plasma may decrease with the time under the US field.

The distributions of character temperatures T_e^*, T_r^*, T_v^* in plasma in the DGCLW working in water at air flow rate $G=55\text{cm}^3/\text{s}$ at currents $I_d=50\text{-}400\text{ A}$ for three different modes: with solid electrodes, with solid cathode + liquid and with liquid cathode + solid anode are presented below in Fig. 29. Here, electronic temperatures $T_e^*(H)$ and $T_e^*(Cu)$ were determined by using relative intensities of atomic lines H_{α} , H_{β} (656.5, 486.1 nm) and Cu I (465.1, 510.5, 515.5, 521.8, 578.2 nm). The vibrational and rotational temperatures, T_v^* and T_r^* were determined by using relative intensities of molecular bands N_2 (C-B) (0-2) at 380.1 nm and (1-3) at 375.1 nm and OH (A-X) (1-0) at 283.1 nm and (2-1) at 288.4 nm.

As is shown in Fig. 29, the DGCLW generates nonisothermal plasma in the whole range of discharge currents. At that, plasma parameters strongly depend on the discharge mode and polarity of electrodes. In common, the temperatures $T_e^*(Cu)$ in the DGCLW with the liquid electrode gradually increase with increasing discharge current, however, for the mode of liquid anode the $T_e^*(Cu)$ are considerably larger than for the mode of liquid cathode. This difference in the values of character temperatures in the discharge modes with the liquid electrodes is also observed for all other plasma components with the exception of $T_e^*(H)$. With the liquid cathode the $T_e^*(H)$ noticeable increases, whereas with the liquid anode the $T_e^*(H)$ slightly decreases. Larger values for character temperatures in plasma of the DGCLW with the liquid cathode for almost all components (except Cu) may be explained by greater energy input in discharge plasma. For $T_e^*(Cu)$, its larger value for the liquid anode follows by the decrease of the absolute intensity of Cu emission lines (if compared with other two modes); this may indicate a reduction in output of Cu from the electrodes in this regime.

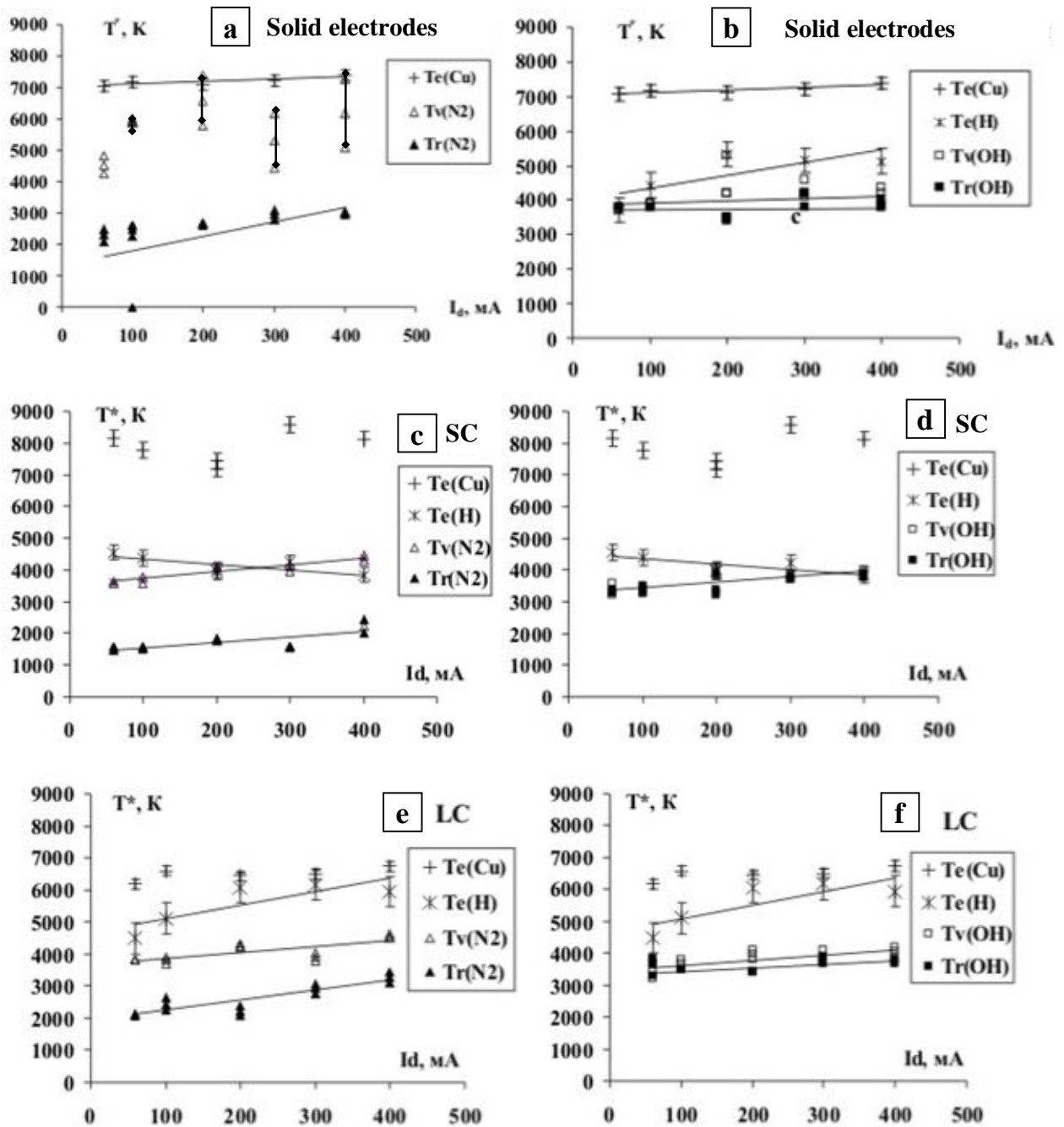


Fig. 29. Character temperatures T_e^*, T_r^*, T_v^* in discharge plasma vs. currents in the DGCLW working in water in different modes: (a, b) with solid electrodes, (c, d) with solid cathode + liquid anode, (e, f) with liquid cathode + solid anode. Air flow rate $G=55 \text{ cm}^3/\text{s}$.

Analyzing the obtained values and dependences, one can conclude that the investigated DGCLW generates nonequilibrium reacting plasma whose parameters are close to nonequilibrium plasma of the gliding arc, which is effectively used in non-thermal atmospheric-pressure plasma-assisted initiation and plasma-supported combustion of hydrocarbon fuels [7].

The results of OES diagnostics of plasma in the DGCLW working in pure ethanol and ethanol/water mixture (5/1) at the air flow rate $G=55\text{cm}^3/\text{s}$ at currents $I_d=50\text{-}400\text{ A}$ in the mode with two solid electrodes are shown in Fig. 30.

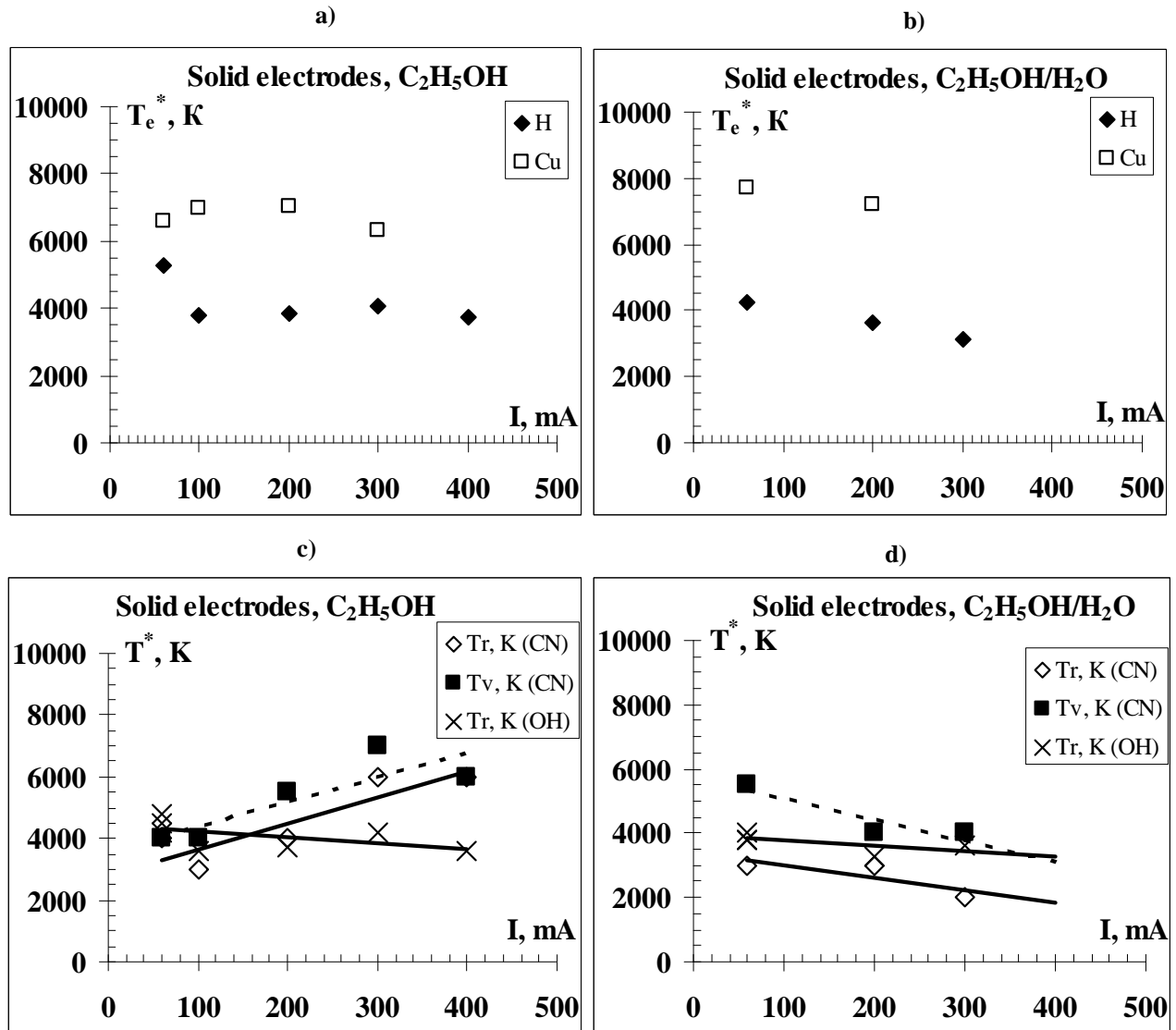


Fig. 30. Character temperatures T_e^*, T_r^*, T_v^* in discharge plasma vs. current in the DGCLW with solid electrodes: (a, c) are pure ethanol, (b, d) are ethanol/water mixture (5/1). Air flow rate $G=55\text{ cm}^3/\text{s}$.

From the temperature dependencies in Fig. 30 one can reveal that the transition from the water to the pure ethanol in the DGCLW does not affect very much character temperatures $T_e^*(\text{Cu})$, $T_e^*(\text{H})$ and $T_r(\text{OH})$, except CN, when noticeable difference between T_r and T_v takes place. The last fact demonstrates the effect of thermalization and reduction of non-equilibrium in plasma. Possible reason may be additional energy input from ethanol due to initiation of combustion processes in the plasma-fuel system.

The results of OES diagnostics of plasma in the DGCLW working in the mode with the liquid anode in ethanol/water mixture (5/1) at the air flow rate $G=55\text{cm}^3/\text{s}$ at currents $I_d=50\text{-}400\text{ A}$ are shown in Fig. 31. From the temperature dependences obtained one can reveal that in the investigated regimes in the DGCLW working with the liquid anode, the characteristic temperatures for radical CN are close $T_v(\text{CN}) \approx T_r(\text{CN})$ and for molecule C_2 are differ $T_v(\text{C}_2) > T_r(\text{C}_2)$. At that, $T_v(\text{CN})$ and $T_r(\text{CN})$ exceed $T_v(\text{C}_2)$ a little bit ($\sim 20\%$). With increasing discharge current from 100 mA to 400 mA, all temperatures are decreased from 4000-5000 K to 3000-4000 K.

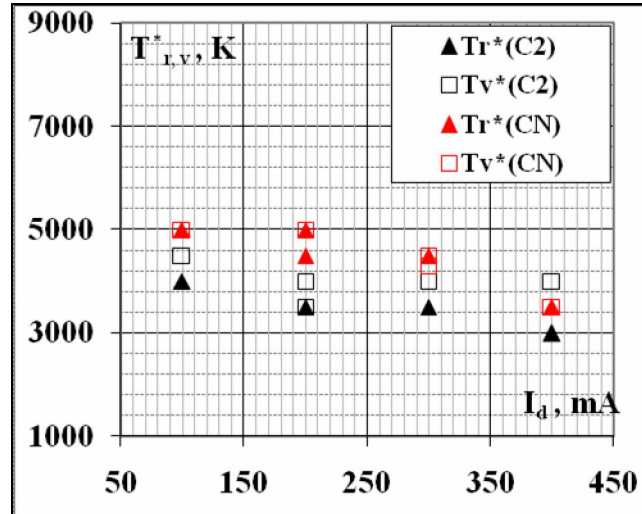


Fig. 31. Character temperatures T_r , T_v in discharge plasma vs. current in the DGCLW with the liquid anode working in ethanol/water mixture (5/1). Air flow rate $G=55\text{ cm}^3/\text{s}$.

Fig. 32 shows the fragments of emission spectra related to the C_2 ($d^3\Pi_g - a^3\Pi_u$) Swan band emission in the spectral range 516-570 nm as obtained in plasma of the DGCLW with the liquid cathode working in ethanol/water mixture (5/1) with and without US field. One can see that fragments are almost identical, so the effect is practically absent. It can be explained by the possible depletion of US cavitations in the work liquid caused by additional gas evolution in plasma-liquid system due to reforming.

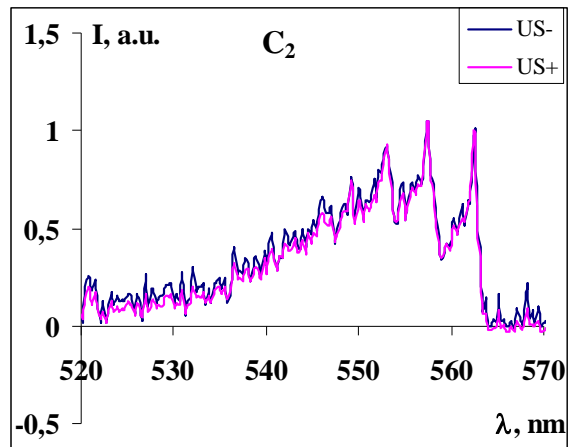


Fig. 32. Spectral distribution of the C_2 ($d^3\Pi_g-a^3\Pi_u$) emission in plasma of the DC DGCLW with liquid cathode working in ethanol/water mixture (5/1) with and without US field. Discharge current $I_d = 100$ mA, air flow rate $G=55$ cm³/s.

The current-voltage and power characteristics of the DC DGCLW working in ethanol-water solution are shown in Fig. 33. A dropping character of I - V curves at discharge currents from 100 to 400 mA indicates the transition regime from the abnormal glow to the arc discharge.

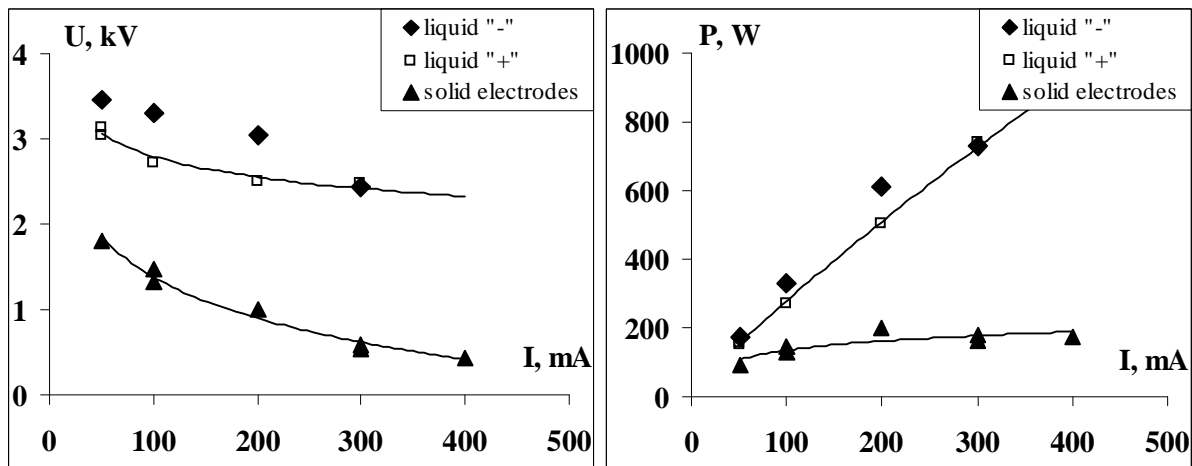


Fig. 33. Current-voltage (left) and power (right) characteristics of the DGCLW working in different modes in ethanol-water solution (5/1). Air flow rate $G= 55$ cm³/s.

The results of mass-spectrometric and gas-chromatographic measurements of concentrations of basic components in output gas products after the ethanol processing in the DGCLW at different discharge currents are shown in Figs. 34-36. These data are given for the case of mixture $C_2H_5OH : H_2O = 5:1$ and airflow rate $G=55 \text{ cm}^3/\text{s}$.

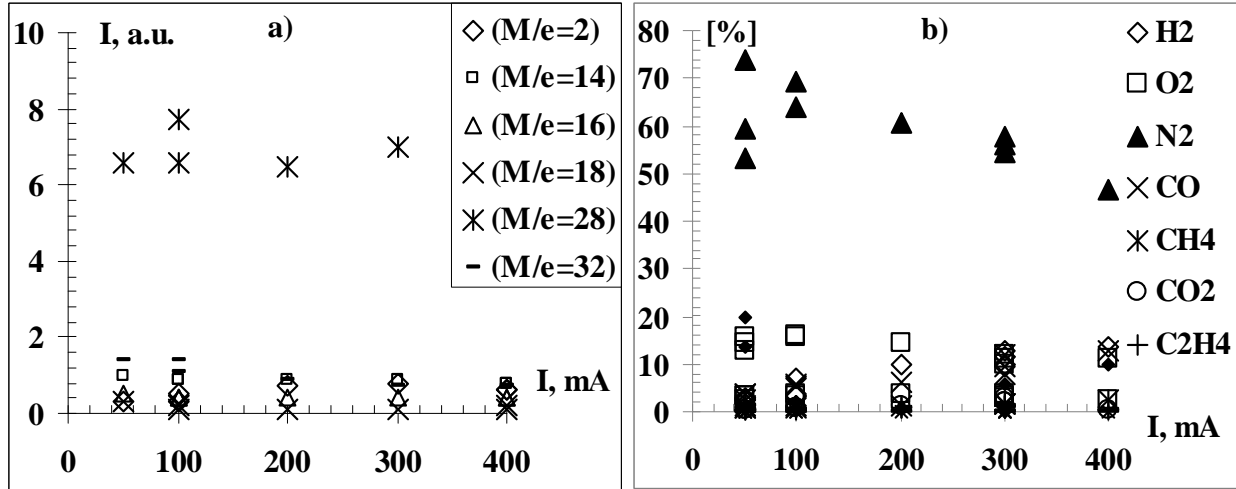


Fig. 34. Data of mass-spectrometry (a) and gas-chromatography (b) analysis of output gas products after the ethanol processing in the DGCLW. The mass ratio $M/e = 2$ is H_2^+ , 12 is C^+ , 14 is N^+ , 16 is O^+ , CH_4^+ , 18 is H_2O^+ , 28 is CO^+ , N_2^+ , and 32 is O_2^+ .

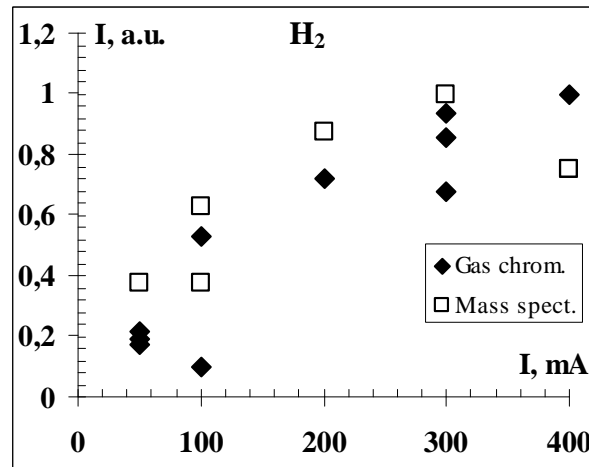


Fig. 35. Content of H_2 in output gas products after the ethanol processing in the DGCLW. Ethanol-water solution (5/1), airflow rate $G=55 \text{ cm}^3/\text{s}$.

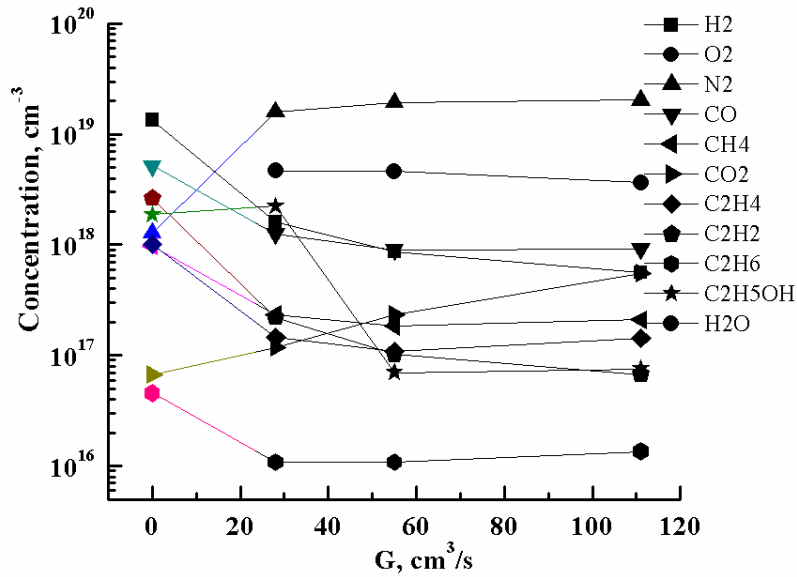


Fig. 36. Concentrations of output gas products after the ethanol processing in the DGCLW as function of air flow rate. Ethanol-water solution (5/1), $I_d=100$ mA.

Fig. 37 shows the results of numerical modeling and calculations of concentrations of H_2 , CO_2 and other main stable components in output gas products after the ethanol processing in the PLS with the DGCLW. The qualitative and quantitative agreement between calculated and measured data is quite good, at least, for main components. One can see that the output concentration $[H_2]$ grows linearly with the discharge current and it reduces exponentially with the gas flow rate.

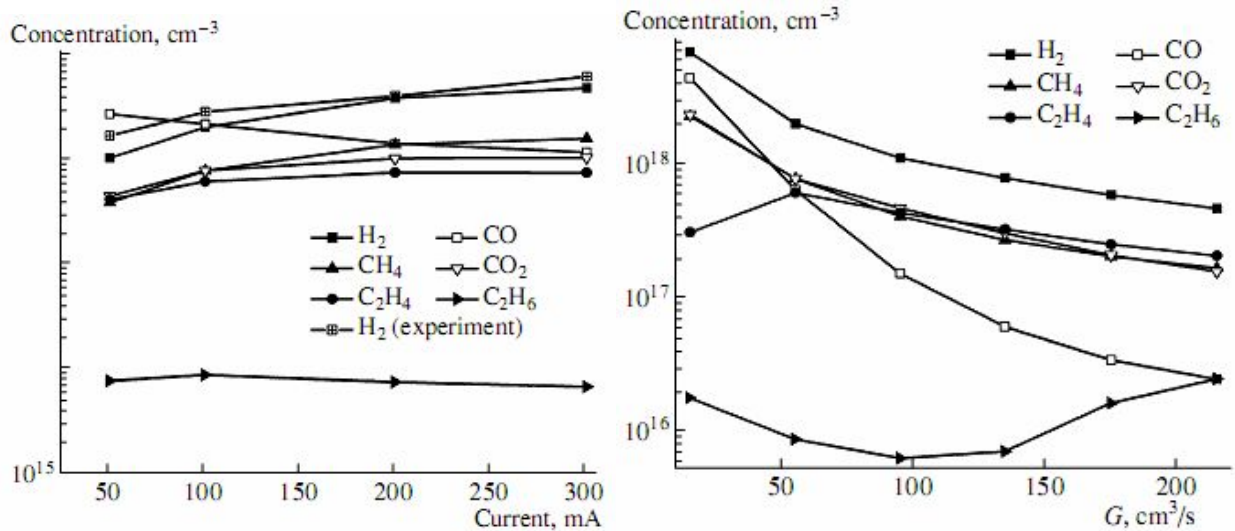


Fig. 37. Calculated concentrations of output gas products after the ethanol processing in the DGCLW as functions of discharge current (left, $G=55$ cm^3/s) and air flow rate (right, $I_d=100$ mA). $C_2H_5OH : H_2O = 5:1$.

In the discharge conditions, the kinetics of the H₂ formation is determined mainly by the reaction $C_2H_5OH + H \rightarrow CH_3CH_2O + H_2$. Since the ethanol concentration [C₂H₅OH] in solution changes slowly, the [H₂] production is determined entirely by the concentration of atomic hydrogen [H].

In the case under consideration, the main process responsible for the generation of H is the dissociation of water molecules H₂O by the direct electron impact. The rate of this process is proportional to the specific electric power deposited to discharge (i.e., discharge current). Therefore, the [H₂] production is also a linear function of the discharge current in accordance with experimental data. Outside the discharge, the only process that influences the H₂ concentration is the water-gas shift reaction $CO + H_2O \rightarrow H_2 + CO_2$. Via this process, the system reaches the complete conversion of CO into CO₂ and H₂.

The estimation of efficiency of the proposed method of the plasma reforming of liquid ethanol into synthesis gas in the PLS-DGCLW reformer was performed on the basis of thermochemical calculations using criteria: (a) energy cost of 1 m³ syngas products; (b) productivity of conversion; (c) specific heat of 1 m³ syngas combustion, and (d) energy efficiency.

Calculations were made with taking into account standard thermochemical constants of hydrocarbons [25] using the formula for the coefficient of energy transformation [16]:

$$\alpha = \frac{\sum_i Y_i \times LHV(Y_i)}{IPE} \quad (3)$$

and also for the conversion efficiency by Fulcheri et al [6]:

$$\eta = \frac{(Y_{H_2} + Y_{CO}) \times LHV(H_2)}{IPE + Y_{HC} \times LHV(HC)} \quad (4)$$

Here, *IPE* is the input plasma energy, *Y* is the molar fraction, *LHV* is the lower heating value of syngas components, *HC* is the hydrocarbon fuel (ethanol). The formula (4) assumes that CO can be totally transformed into H₂ by the water-gas shift reaction with zero energy cost.

The results of estimations in the form of $\alpha(I)$ and $\eta(I)$ dependencies for the ethanol reforming in the DGCLW for different discharge modes against the discharge power are presented in Fig. 38.

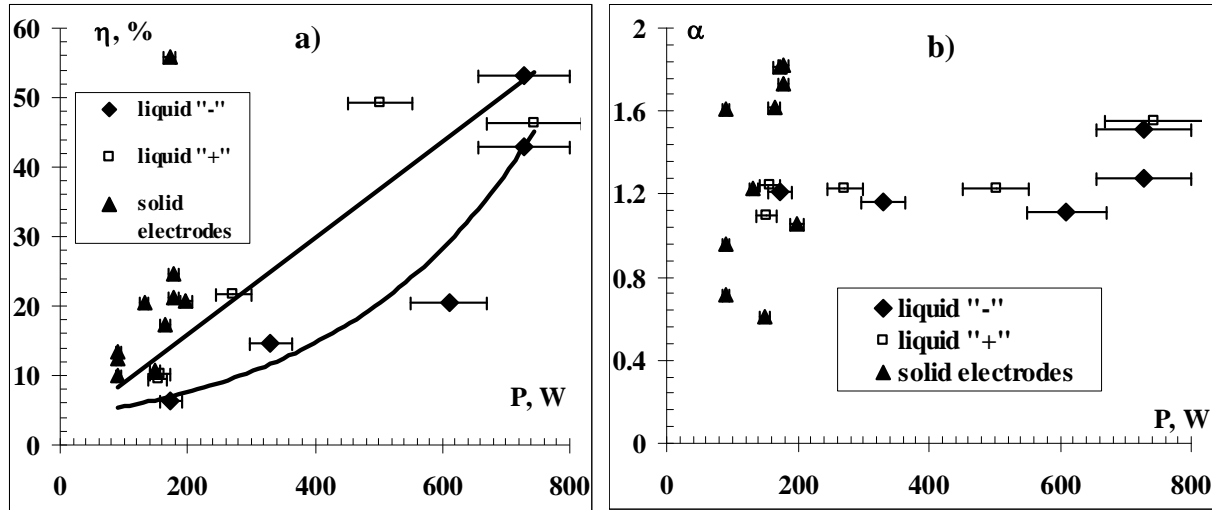


Fig. 38. Dependencies of (a) efficiency of conversion η and (b) coefficient of energy transformation α for the ethanol reforming in the DGCLW in different discharge modes as a function of the discharge power (currents vary from 50 to 400 mA). $C_2H_5OH : H_2O = 5:1$.

One can see that the net H_2 yield in the discharge at $I = 300$ mA is $\sim 15\%$ whereas the energy efficiency of the ethanol conversion into the syngas is up to 50%. (input energy is 4-10% of $LHV = 26.8$ MJ/kg). These numbers correlate with our earlier results [27, 28] and are comparable with other known plasma-aided ethanol reforming methods [6].

Fig. 39 shows the values of coefficient α and parameter η together with data of mass-spectrometry of H_2 in the DGCLW for different modes at different discharge currents. One can see that that the coefficient α for the mode of solid electrodes has the same growth trend with increasing current as the H_2 yield. And for modes of liquid electrode the parameter of efficiency η has the same trend of growth as the H_2 yield.

This difference in behavior of parameters may be caused due to the fact that the power of discharge using the liquid electrode is proportional to the current. At smaller currents the efficiency is of 20%, at large currents the efficiency is at 45-55%. For the modes of liquid electrode with increased current the level of efficiency of reforming is higher than for the mode of solid electrodes. At that, each mode demonstrates increased efficiency with increasing current.

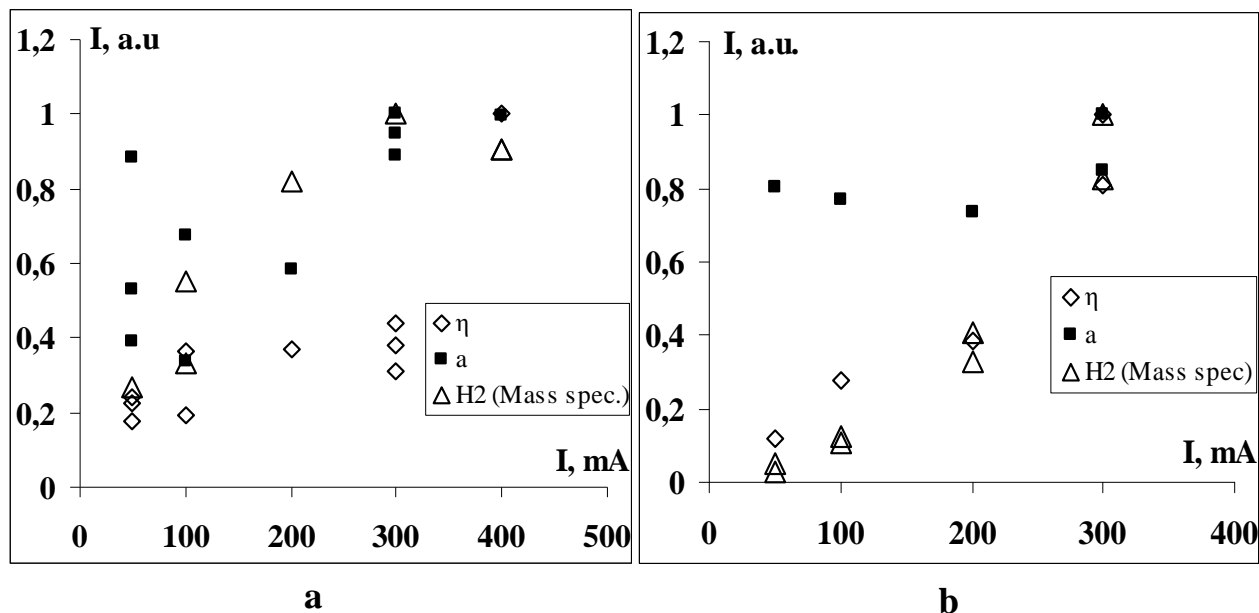


Fig. 39. Coefficient of energy transformation α , conversion efficiency η and H₂ yield as measured by mass-spectrometry for the ethanol reforming in the DGCLW at different currents: a) mode of solid electrodes; b) mode of liquid cathode.

The impact of the plasma-forming gas on the ethanol reforming in the DGCLW was also studied. For that, the composition of gas-phase products of conversion in the reactor and the coefficient of energy transformation were studied at different gas flow rates. Research was conducted for the mode of solid electrodes. The composition and mixture ratio under the ethanol reforming were taken the same as in previous research. The discharge current varied between 100 and 400 mA, the air flow rate varied from 0 to 110 cm³/s.

Fig. 40 shows the results for $I = 100$ mA that demonstrates a good matching between gas chromatography and mass-spectrometry data. For other currents the same matching is observed. It should be noted that with increasing air supply in the discharge the concentration of H₂ in syngas products decreases. In fact, the highest yield of H₂ is observed in the discharge mode without air supply. But the time of H₂ production in this case increases considerably, and the power consumption also increases. All this reduces the coefficient of energy transformation (Fig. 41). Moreover, this decreases the lifetime of the system. Therefore, the total system performance without air supply seems to be not very good.

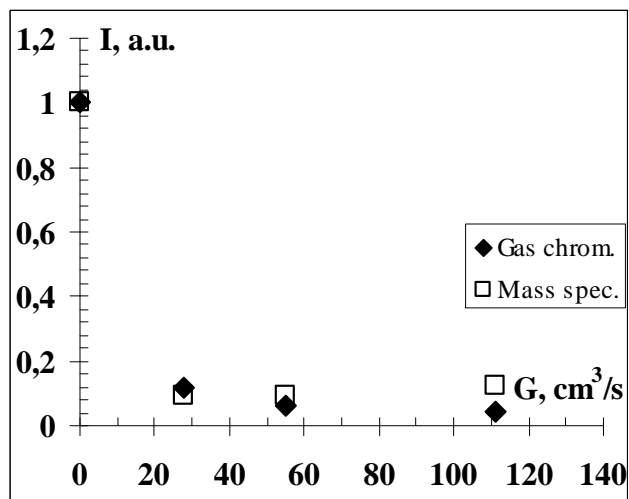


Fig. 40. H₂ measured by gas-chromatography and mass-spectrometry after the reforming in the DGCLW with solid electrodes at different air flow rates. $I_d = 100$ mA.

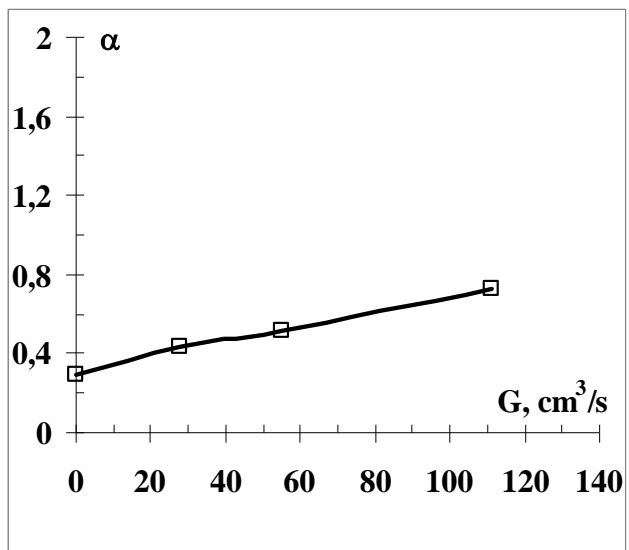


Fig. 41. Coefficient of energy transformation α for the ethanol reforming in the DGCLW with solid electrodes at different air flow rates. $I_d = 100$ mA.

The results of the studies of the postdischarge pyrolysis of ethanol after initial plasma-assisted ethanol reforming are presented in Figs. 42-43. The experimental parameters were following: discharge frequency 420 Hz, air flow rate 17-28 cm³/s, time of treatment up to 10 min (600 s); the temperature in the pyrolytic chamber varied from 0 to 870 K. The principal feature of the pulsed discharge power supply in comparison with dc mode is the ability to work with higher energy input in plasma at comparable power capacity. This gives more intensive plasma stimulation of pyrolysis due to deep injection of plasma in the pyrolytic chamber.

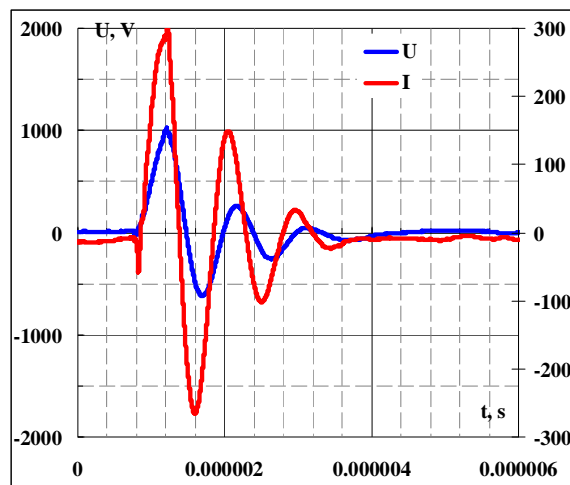


Fig. 42. Voltage and current oscillograms in the pulsed DGCLW.

Fig. 43 shows the H₂ as measured by mass-spectrometry and partial H₂ content in syngas as measured by gas-chromatography after the ethanol pyrolysis in a pyrolytic chamber. One can see a good correlation between GC and MS data. Also noticeable that the H₂ production in the pyrolytic chamber without discharge is very low (indicated by empty signs).

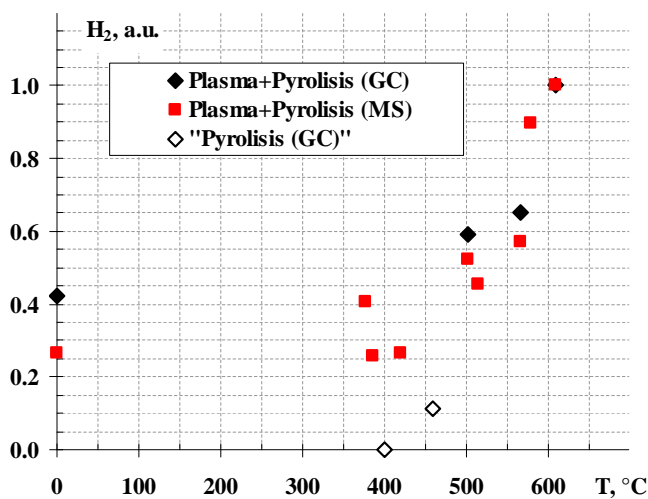


Fig. 43. H₂ as measured by mass-spectrometry and partial H₂ content in syngas as measured by gas chromatography after the ethanol pyrolysis vs. temperature in the pyrolytic chamber.

Fig. 44 shows the coefficient of energy transformation α for the reforming system as a function of temperature in the pyrolytic chamber. It is seen that values α increase with increasing temperature. Some modes with the change of air flow (modes 5+2 and 5+3 correspond to additional air supply into the pyrolytic chamber comparably with the air supply in the discharge) have lower energy efficiency than the mode with the constant air flow because of variation of partial output of isobutane iC_4H_{10} . Fig. 45 shows the rate of syngas production in the reforming system. One can conclude that the investigated combination of electric discharge + postdischarge pyrolysis for the ethanol reforming demonstrates the smart efficiency of this approach.

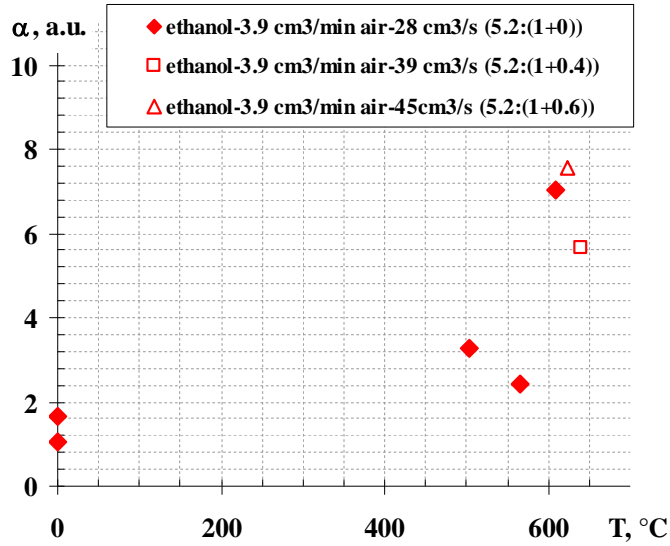


Fig. 44. Coefficient of energy transformation α vs. temperature in the pyrolytic chamber.

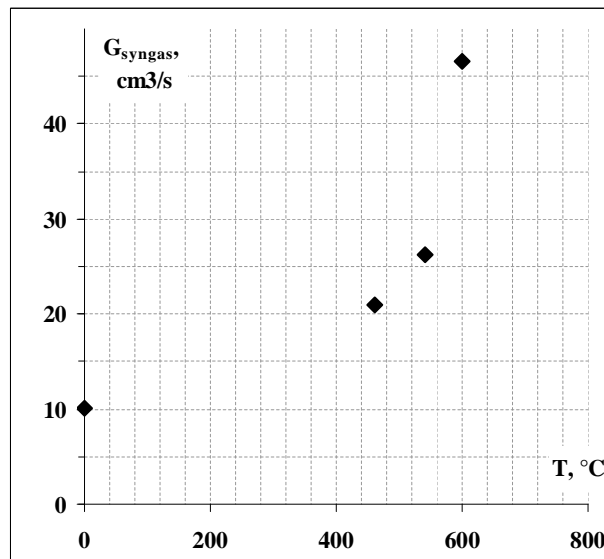


Fig. 45. The rate of syngas production vs. temperature in the pyrolytic chamber.

Among possible systems that can efficiently inject plasma into the pyrolytic chamber, one of the most prospective is the discharge in a reverse vortex flow of Tornado type that can generate the high-speed vortex jets of plasma of atmospheric pressure.

We have prepared the PLS reactor with the DC discharge in a reverse vortex gas flow of Tornado type with the "liquid" electrode (TORNADO-LE) as is shown in Fig. 46. It consists of a cylindrical quartz vessel (1) by diameter of 9 cm and height of 5 cm, sealed by the flanges at the top (2) and at the bottom (3). The vessel was filled by the work liquid (4) through the inlet pipe (5) and the level of liquid was controlled by the spray pump. The basic cylindrical T-shaped stainless steel water-cooled electrode (6) on the lower flange (3) made from stainless steel is fully immersed in the liquid. The electrode on the upper flange (2) made from duralumin had a special copper hub (11) with the axial nozzle (7) by diameter 2 mm and length of 6 mm. The gas was injected into the vessel through the orifice (8) in the upper flange (2) tangentially to the cylinder wall (1) and created a reverse vortex flow of tornado type, so the rotating gas (9) went down to the liquid surface and moved to the central axis where flowed out through the nozzle (7) in the form of jet (10) into the quartz chamber (12). Since the area of minimal static pressure above the liquid surface during the vortex gas flow is located near the central axis, it creates the column of liquid at the gas-liquid interface in the form of the cone with the height of ~1 cm above the liquid surface (without electric discharge).

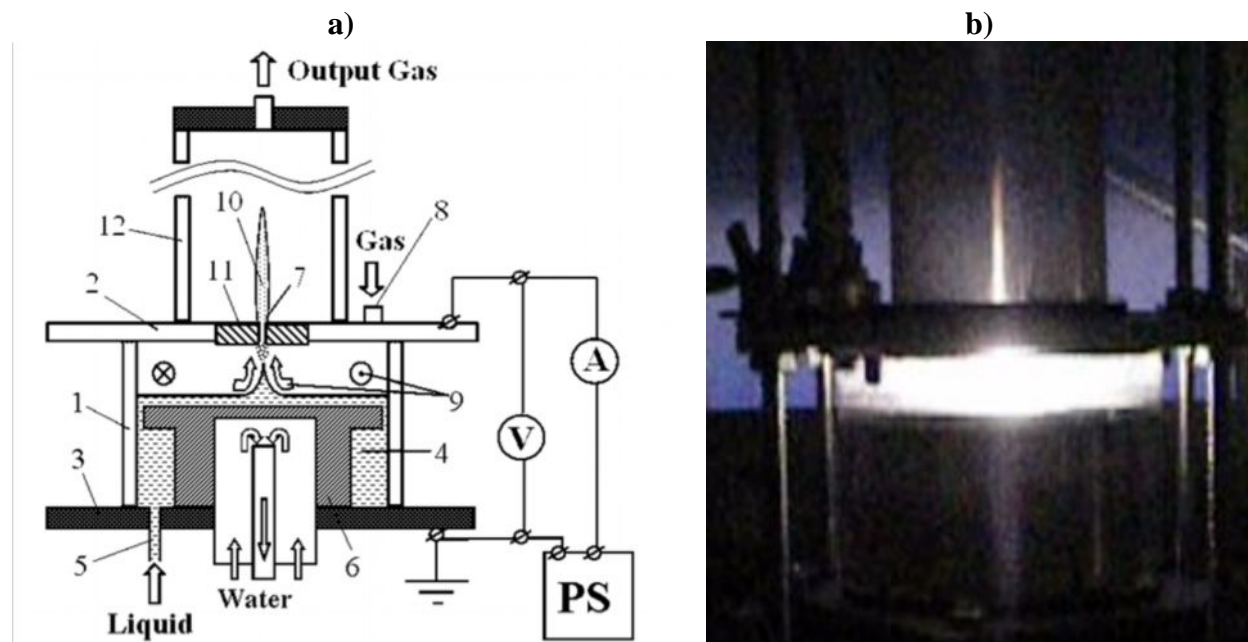


Fig. 46. Schematic (left) of the PLS reactor with the DC discharge in a reverse vortex gas flow of Tornado type with a "liquid" electrode and photo (right) of the TORNADO-LE working in ethanol-water solution.

The voltage was supplied between the upper electrode (2) and the lower electrode (6) in the liquid with the help of the DC power source powered up to 10 kV. Two modes of the discharge operation were studied: the mode with "liquid" cathode (LC) and the mode with "liquid" anode (LA): "+" is on the flange (2) in the LC mode, and "-" is on the flange (2) in the LA mode. The conditions of breakdown in the discharge chamber were regulated by three parameters: by the

level of the work liquid; by the gas flow rate G ; and by the value of voltage U . The ignition of discharge usually began from the appearance of the axial streamer; the time of establishment of the self-sustained mode of operation was $\sim 1-2$ s. The range of discharge currents varied within 100-400 mA. The pressure in the discharge chamber during the discharge operation was ~ 1.2 atm, the static pressure outside the reactor was ~ 1 atm. The elongated ~ 5 cm plasma torch (10) was formed during the discharge burning in the camera.

The typical current-voltage characteristics of the TORNADO-LE with the liquid anode working in water at different airflow rates are shown in Fig. 47.

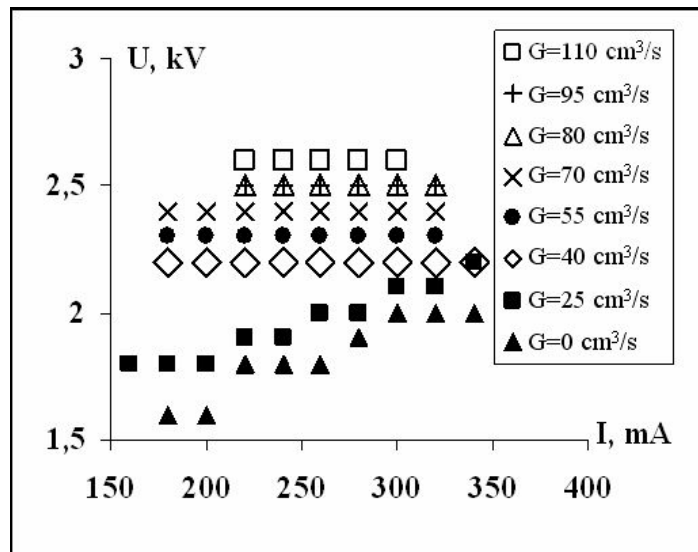


Fig. 47. Current-voltage characteristics of TORNADO-LE with the liquid anode working in ethanol-water solution at different airflow rates.

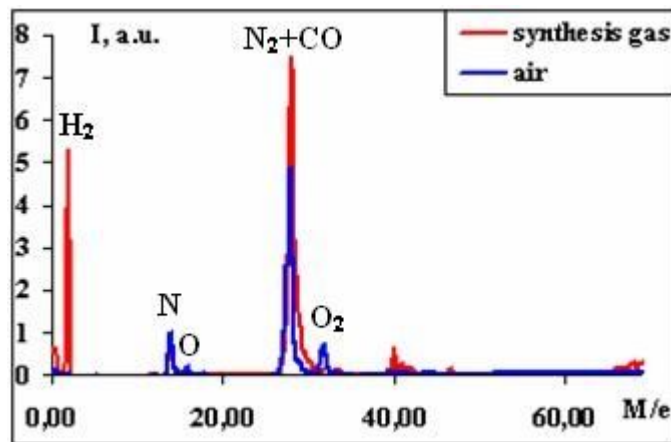


Fig. 48. Mass-spectrometry of gas products after the reforming in the TORNADO-LE with liquid cathode. Voltage 2 kV, current 320 mA, air flow rate $55 \text{ cm}^3/\text{s}$, mixture $\text{C}_2\text{H}_5\text{OH}/\text{H}_2\text{O} = 1/4$.

Results of mass-spectrometry of output syngas products after the ethanol reforming in the TORNADO-LE are shown in Fig. 48. One can see that content of H₂ and CO in output syngas products is quite high.

The estimated coefficients of energy transformation for the ethanol reforming in the PLS with the TORNADO-LE depending on the initial ethanol concentration in the ethanol-water mixture are presented in Fig. 49. One can see that values α are quite high and reach ~0.8 at 25% ethanol-water solution.

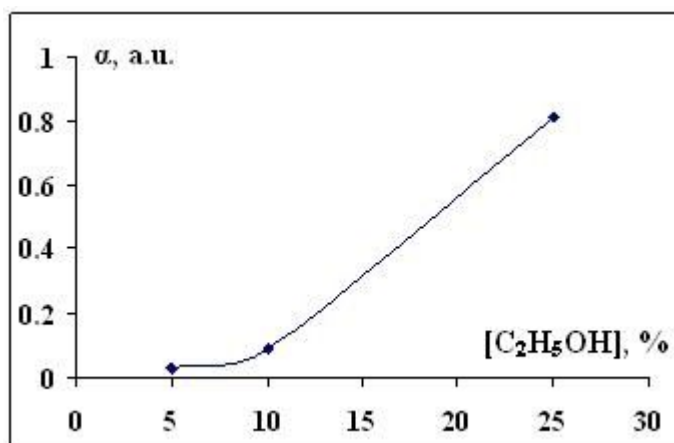


Fig. 49. Coefficient of energy transformation for the ethanol reforming in the TORNADO-LE as a function of the initial ethanol concentration.

Thus, our results of preliminary studies demonstrate that the glow discharge in the reverse vortex flow of Tornado type with the liquid electrode is very perspective for the plasma-assisted reforming of liquid hydrocarbon fuels.

Future Work

We are planning the following research activities in the future:

- To study the regimes and parameters of non-thermal plasma reforming of liquid fuels in the pulsed discharge in a gas channel with liquid wall.
- To study the regimes and parameters of non-thermal plasma reforming of liquid fuels in the plasma-liquid system with reverse vortex flow using pulse and DC discharge of tornado type with “liquid” electrode.
- To study the reforming of liquid hydrocarbons in plasma-liquid systems with microporous media (liquid+microbubbles) and aerosols (gas+microdroplets) using low-frequency (~20 kHz) and high-frequency (~800 kHz) ultrasound.
- To study the regimes and parameters of plasma-supported combustion of paraffin fuels by using gas dynamic electric discharges.

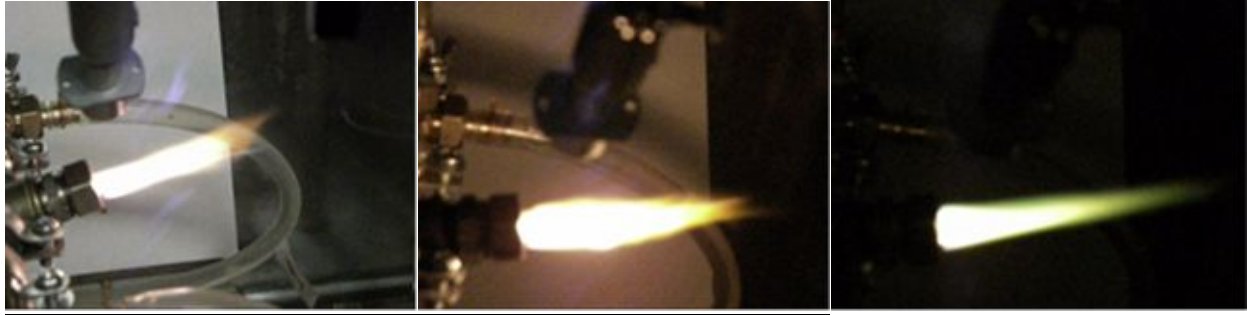


Fig. 50. Photo images of the first test of plasma-assisted paraffin combustion as demonstrated in the plasma-chemical laboratory of the KNU in Kiev by April 2010.

Publications

As a result of the project activity during the year, at least, 4 papers were published in peer-reviewed journals including the topic issue of IEEE Trans. Plasma Sciences, 1 report was presented in the program of the 3rd European Conference of Aero-Space Sciences – EUCASS 2009 in ONERA, Paris, France, 9 reports at the 3rd Central European Symposium on Plasma Chemistry – CESPC 2009 in KNU, Kiev, Ukraine, 1 report at the XVIII Symp. on Physics of Switching Arc 2009 in Nové Město na Moravě, Czech Republic, 1 report in the VI Intern. Conf. on Plasma Physics and Plasma Technology 2009 in Minsk, Belarus, etc.

The key references are:

1. Chernyak V.Ya., Olszewskii S.V., Yukhymenko V.V., Solomenko E.V., Prysiazhnevych I.V., Naumov V.V., Levko D.S., Shchedrin A.I., Ryabtsev A.V., Demchina V.P., Kudryavtsev V.S., Martysh E.V., and Verovchuk M.A. Plasma-assisted reforming of ethanol in dynamic plasma-liquid system: experiments and modeling // IEEE Trans. Plasma Sci. Vol. 36, Dec. 2008, p. 2933-2939.
2. Chernyak V., Olszewski S., Prysiazhnevych I., Yukhymenko V., Shapoval V., Naumov V., Levko D., Shchedrin A., Rybatsev A., Demchina V., and Kudryavtsev V. Transversal gas discharges in plasma liquid systems and its applications for environmental protection // Przegląd elektrotechniczny (Electric Review. ISSN 0033-2097). R.85 NR 5/2009. p.144-147.
3. Yukhymenko V.V., Verovchuk M.O., Olszewskii S., Chernyak V.Ya., Zrazhevskij V.A., Demchina V.P., Kudryavzev V.S., Shchedrin A.I., Levko D.S., and Naumov V.V. Conversion of ethanol in dynamic plasma-liquid system // Problems Atomic Sci. Technology, Series: Plasma Physics, Vol. 15, 2009, N1, p.128-130.
4. Shchedrin A.I., Levko D.S., Chernyak V.Ya., Yukhimenko V.V., Naumov V.V., Conversion of air mixture with ethanol and water vapors in nonequilibrium gas-discharge plasma // Tech. Phys. Lett. Vol. 35, 2009, p. 449-451.
5. Chernyak V.Ya., Yukhymenko V.V., Prysiazhnevich I.V., Olszewskii S.V., Shchedrin A.I., Levko D.S., Naumov V.V., Sidoruk S.M., Verovchuk M.O., Demchina V.P., Kudryavzev V.S., Generation of hydrogen in system with the electrical discharge in the air channel inside liquid fuel // Proc. 3rd European Conf. for Aero-Space Sciences – EUCASS 2009, July 6-9, Paris, France, ONERA, 2009.
6. V. Yukhymenko, V. Chernyak, S. Olszewskii, M. Verovchuck, D. Levko, A. Shchedrin, V. Demchina, V. Kudryavtsev. Experimental study and theoretical modeling of process of

- ethanol reforming into synthesis gas in DGCLW // 19th Intern. Symp. on Plasma Chemistry, Bochum, July 26-31, 2009, Proceedings #P2.14.30.
7. O. Lomonos, I. Prysiazhnevych, V. Chernyak, V. Yukhymenko, S. Olszewski, Methods of vibration and rotation temperature determining for plasma of DGCLW by using OH (A-X) band // Proc. 9th Int. Young Sci. Conf. on Applied Physics, June 17-20, 2009, Kyiv, Ukraine, p.94.
 8. Ol. Solomenko, S. Olszewski, I. Prysiazhnevych, V. Chernyak, Properties of plasma-liquid with microporous system based on the discharge in gas channel with liquid // Proc. 9th Int. Young Sci. Conf. on Applied Physics, June 17-20, 2009, Kyiv, Ukraine, p.93.
 9. M.O. Verovchuk, V.V. Yukhymenko, V.Ya. Chernyak, I.V. Prysiazhnevych, Optical spectroscopy of transverse arc discharge in a mix flow of air and ethanol // Proc. 9th Int. Young Sci. Conf. on Applied Physics, June 17-20, 2009, Kyiv, Ukraine, p.92.
 10. S. Olszewski, Ol. Solomenko, I. Prysiazhnevych, V. Chernyak, Properties of plasma microporous-liquid system // Proc. 9th Int. Young Sci. Conf. on Applied Physics, June 17-20, 2009, Kyiv, Ukraine, p.81.
 11. Ok. Solomenko, V. Chernyak, I. Prysiazhnevych, Ja. Diatczyk, H. Stryczewska, Modelling of transition metals emission spectra registered by spectrometers with low spectral resolution // Proc. 9th Int. Young Sci. Conf. on Applied Physics, June 17-20, 2009, Kyiv, Ukraine, p.82.
 12. D. Levko, A. Shedrin, V. Chernyak, V. Yukhymenko, V. Naumov, Conversion of ethanol in plasmachemical reactor in regime with one solid electrode // Proc. 9th Int. Young Sci. Conf. on Applied Physics, June 17-20, 2009, Kyiv, Ukraine, p.83.
 13. Shchedrin A.I., Levko D.S., Chernyak V.Ya., Yukhymenko V.V., Naumov V.V. Plasma kinetics in electrical discharge in mixture of ethanol with air in plasma chemical reactor in regime with one solid electrode // III CESPC, Aug. 23-27, 2009, Kyiv, Ukraine. -P.67-68.
 14. Shchedrin A.I., Levko D.S., Chernyak V.Ya., Yukhymenko V.V., Naumov V.V. Plasma kinetics in electrical discharge in mixture of ethanol with air in plasma chemical reactor in regime with both solid electrodes // III CESPC, Aug. 23-27, 2009, Kyiv, Ukraine.-P.89-90.
 15. Sidoruk S.S., Chernyak V.Ya., Olszewski S.V. Pulsed discharge in a gas channel with liquid wall // III CESPC, Aug. 23-27, 2009, Kyiv, Ukraine. - P.92-93.
 16. Prysiazhnevych I.V., Lomonos O.I., Chernyak V.Ya., Yukhymenko V.V., Olzewski S.V. Plasma parameters of the atmospheric pressure discharge in air channel with water wall // III CESPC, Aug. 23-27, 2009, Kyiv, Ukraine. - P. 96-97.
 17. Yukhymenko V.V., Chernyak V.Ya., Verovchuk M.O. Reforming of ethanol in plasma - liquid system with discharge in gas channel with liquid wall // III CESPC, Aug. 23-27, 2009, Kyiv, Ukraine, - P. 98-99.
 18. Olszewski S., Solomenko Ol., Yukhymenko V., Chernyak V. Combined affecting of ultrasonic field and plasma discharge in gas channel with liquid wall to the water-phenol solutions // III CESPC, August 23-27, 2009, Kyiv, Ukraine, - P. 100-101.
 19. Olszewski S., Solomenko O., Prysiazhnevych I., Chernyak V. Combined affecting of ultrasonic field and plasma discharge in gas channel with liquid wall to the distilled water // III CESPC, Aug. 23-27, 2009, Kyiv, Ukraine. - P. 102-103.
 20. Yukhymenko V.V., Verovchuk M.O., Chernyak V.Ya., Prysiazhnevych I.V., Naumov V.V. Properties of the transversal arc plasma in air + ethanol mixture// III CESPC, Aug. 23-27, 2009, Kyiv, Ukraine. - P. 108-109.

21. Levko D.S., Shchedrin A.I., Chernyak V.Ya., Yukhymenko V.V., Naumov V.V. The use of non-equilibrium plasma for ethanol conversion // All-Ukr. Conf. on Plasma Physics and Controlled Fusion, 27-28 Oct. 2009, Kiev, Book of Abstracts, P. 23.
22. Safonov E.K., Chernyak V.Ya., Olzewski S.V., Prysiashnevych I.V. Plasma-liquid systems with gas-dynamic quenching // III CESP, Aug. 23-27, 2009, Kyiv, Ukraine. - P. 166-167.
23. Chernyak V., Olzewski S., Prysiashnevych I., Yukhymenko V., Levko D., Shchedrin A., Rybatsev A., Naumov V., Demchina V., Kudryavtsev V. Plasma-liquid systems with transversal discharges // Proc. XVIII Symp. on Physics of Switching Arc, Sept. 7-11, 2009, Nové Město na Moravě, CR, p. 29-38.
24. Chernyak V.Ya., Yukhymenko V.V., Prysiashnevych I.V., Olzewski S.V., Sidoruk S.M., Verovchuk M.O., Shchedrin A.I., Levko D.S., Demchina V.P., Kudryavtsev V.S. Using of combined electrical discharge in the air channel inside to the water-organic solutions for generation of hydrogen // Proc. VI Intern. Conf. on Plasma Physics and Plasma Technology. 28 Sept.-2 Oct. 2009, Minsk, Belarus. Contrib. Papers. p. 851-854.
25. Chernyak V.Ya., Yukhymenko V.V., Olzewskii S.V., Prysiashnevych I.V., Sydoruk S.M., Verovchuk M.A., Shchedrin A.I., Levko D.S., Naumov V.V., Demchina V.P., Kudryavtsev V.S., Electric discharge plasma reforming of liquid hydrocarbons into hydrogen for use in aerospace technologies // Modern science: studies, ideas, results,, technologies. - 2009. N.2 (special issue "Ukrainian Workshop on Aerospace Technologies). p. 6-7.
26. Chernyak V., Olzewskii S., Nedybalyuk O., Sydoruk S., Yukhymenko V., Prysiashnevych I., Shchedrin A., Levko D., Naumov V., Demchina V., Kudryavtsev V. Plasma Reforming of Ethanol in Dynamic Plasma-Liquid Systems // Proc. 10th Intern. Conf. on Combustion and Energy Utilization – ICCEU 2010, 3-8 May 2010, Mugla, Turkey. - P. 295-300.
27. Chernyak V.Ya., Olzewski S.V., Yukhymenko V.V., Nedybalyuk O.A., Sydoruk S.M., Prysiashnevych I.V., Levko D.S., Shchedrin A.I., Filatov S.A., Veremij Yu.P., Demchina V.P. Plasma-liquid systems with transversal electrical discharges and its applications // Abstracts Intern Conf. "Physics of liquid matter: modern problems, May 21-24, 2010, Kyiv, Ukraine. – P. 284.
28. Prysiashnevych I.V., Chernyak V.Ya., Yukhymenko V.V., Olzewski S.V., Solomenko O.V., Lomonos O.I., Lisitchenko T.E. Plasma-liquid system with discharge in the air channel with water wall // Abstracts Intern Conf. "Physics of liquid matter: modern problems, May 21-24, 2010, Kyiv, Ukraine. – P. 226.
29. Yukhymenko V.V., Chernyak V.Ya., Olzewskii S.V., Sidoruk S.M., Demchina V.P., Levko D.S., A.I. Shchedrin. Plasma reforming of fuels in plasma-liquid system // Abstracts Intern Conf. "Physics of liquid matter: modern problems, May 21-24, 2010, Kyiv, Ukraine. – P. 276.
30. Sidoruk S.S., Chernyak V.Ya., Olzewski S.V. Physical properties of pulsed plasma-liquid system // Abstracts Intern Conf. "Physics of liquid matter: modern problems, May 21-24, 2010, Kyiv, Ukraine. – P. 219.
31. Nedybaliuk O.A., Olzewski S.V., Chernyak V.Ya., Lomonos O.I., Shiht I.G. Physical properties of plasma-liquid system with reverse vortex flow // Abstracts Intern Conf. "Physics of liquid matter: modern problems, May 21-24, 2010, Kyiv, Ukraine. – P. 281.
32. Olzewski S.V., Solomenko O.V., Chernyak V.Ya. Properties of discharge in gas channel with liquid wall under ultrasound field // Abstracts Intern Conf. "Physics of liquid matter: modern problems, May 21-24, 2010, Kyiv, Ukraine. – P. 213.

CONCLUSIONS

1. Experimental facilities and laboratory modules of gas-liquid plasma-chemical reactors for plasma reforming of liquid hydrocarbon fuels utilizing the electric discharge in a gas channel with liquid wall are prepared and tested.
2. Experimental methods of modeling and diagnostics including optical emission and absorption spectroscopy, mass spectrometry, gas chromatography, calorimetry and other are selected and tested.
3. Original methods for determining of excitation temperatures in nonequilibrium plasmas of atmospheric pressure discharges by using the SPECAIR code are proposed and tested. To simplify the experimental spectra processing a set of calibration curves for the OH ($A^2\Sigma-X^2\Pi$) and N_2 ($C^3\Pi_u-B^3\Pi_g$) emission bands are calculated and plotted. The proposed approach is efficiently applied for determining of vibrational and rotational temperatures through other molecular bands, CN ($B^2\Sigma^+-X^2\Sigma^+$) and C_2 ($d^3\Pi_g-a^3\Pi_u$). The only disadvantage of this method is the necessity to take into account the form of the instrumental function of the used spectrometer during the calibration curves calculation. It was concluded that suggested approach is universal but the calibration curves obtained in this work are valid only for the certain instrumental broadening.
4. The suggested technique is applied for determining of plasma parameters in the plasma-liquid system with the discharge in a air channel with water wall. It is shown that plasma in the investigated regimes is non-thermal: $T_e^*(Cu) > T_e^*(H) \geq T_v^*(N_2) \approx T_v^*(OH) \geq T_r^*(OH) > T_r^*(N_2)$. The observed discrepancy between electronic temperatures of Cu and H atoms is explained by the additional mechanism of population of the excited electronic states of Cu atoms due to the electron-ion recombination. The observed discrepancy between rotational temperatures determined by the OH (A-X) and N_2 (C-B) bands is not well understood and needs further careful examination.
5. The study of emission spectra of plasma in the blowing transverse arc discharge in a regime of the plasma-assisted fuel combustion in the system of utilization of syngas products after the plasma fuel reforming has shown the following:
 - significant differences in distributions of intensities of spectral atomic lines and molecular bands in the plasma plume along the flow depending on the fuel presence in the air flow. The addition of fuel in the mixture reduces the maxima in the distributions.
 - considerable influences on distributions of electronic temperatures T_e^* of atomic species (H, O) and vibrational T_v^* and rotational T_r^* temperatures of molecular species (N_2 , OH, CN, C_2) in the plasma plume along the flow from both the electrode materials (Cu) and the components of air/fuel mixture (O, N, H). All of them correlate within the measurement uncertainty approximating by linear dependences. Their relationships indicate the changes of the level of non-isothermality of the plasma plume along the flow with the increase of the fuel fraction in the initial mixture.
6. The study of the plasma-liquid system with the discharge in a gas channel with liquid wall in the microporous media under the ultrasound cavitations has shown the following:
 - The action of the ultrasound field in the liquid phase increases the efficiency of the nitrous acid production in the work liquid approximately in 1.5 times.
 - The ultrasound field in the work liquid influences differently on the content of the emission spectra of discharge plasma. Thus, a part of the emission of OH radicals is reduced comparably to the emission of N_2 molecules. There was a linear increasing of

relative intensities of H atoms emission with the time of plasma-liquid processing. But the presence of the ultrasound field reduces this rate approximately in 1.5 times.

7. The comparison of the developed method of numerical modeling of kinetics in air-water-plasma of atmospheric pressure in the plasma-liquid system in the electrical discharge in the gas channel with liquid wall using the assumption of the averaging of the energy that is deposited in the discharge volume without micro-details of the temporal-spatial structure of the discharge and other method of calculations of plasma kinetics in micro-discharges based on the assumption of the multi-channeling of the current in the plasma volume has shown that both approaches give good results in calculations of the component content and concentrations of main components.
8. The main components of syngas produced from ethanol in the PLS-DGCLW reactor are molecular hydrogen H_2 and carbon monoxide CO, which relative yield is many times higher than for hydrocarbons CH_4 , C_2H_2 , C_2H_4 , and C_2H_6 .
9. The composition content of syngas and the power inputs on the ethanol conversion in the DGCLW discharge depends on the initial gas that forms the plasma and on the ethanol-water ratio in the solution.
10. The output hydrogen concentration grows linearly with discharge current.
11. The kinetic plasma-chemical modeling is in a fairly good agreement with experimental data, at least, for the main syngas components, H_2 and CO, predicting a non-thermal plasma-chemical mechanism of the ethanol conversion in the investigated plasma-liquid system.
12. The combination of electric discharge plasma-assisted ethanol reforming and post-discharge pyrolysis of ethanol for hydrogen-rich syngas production is proposed and tested. The synergetic effect of increasing of total energy efficiency of fuel reforming is demonstrated.
13. The PLS system with the glow discharge in the reverse vortex flow of Tornado type with the liquid electrode is proposed and tested. Preliminary results of plasma-assisted reforming of ethanol-water solutions have demonstrated rather high efficiency of fuel conversion and energy transformation.
14. Recommendations to implementation of project results for applications in prospective plasma-assisted aerospace combustion technologies are proposed (“Future work”).

Thus, at this stage of the project research we completed investigations of the process of plasma-assisted conversion of model fuel – ethanol according to the planned research tasks under the undertaken project program.

On the whole, this work has made a great contribution toward achievement of the project objectives aimed to develop a basis for new technology of non-thermal plasma fuel reforming, providing a necessary base for logic continuation of researches further in a way of elaboration of new and advanced (as compared to world achievements) plasma-aided processes based on the state-of-the art technologies in this field.

In conclusion, the investigations in this project discovered many interesting and important regularities of the process of reforming of liquid hydrocarbons in plasma-liquid systems with electric discharges in a gas channel with liquid wall and revealed the main directions in research and developments aimed to create compact and efficient electric reformers for on-board reforming of bio-fuels into hydrogen-rich synthesis gas for applications in prospective aerospace plasma-assisted combustion technologies.

ACKNOWLEDGEMENTS

Publications resulting from the research under this project are presented with the acknowledgements of the STCU, AFOSR and EOARD support.

UA researchers are deeply appreciative to Dr Julian M. Tishkoff and other AFOSR-AFRL scientists for initiation of scientific collaboration and possibilities of interaction.

REFERENCES

1. Warnatz J., Maas U., Dibble R.W. *Combustion. Physical and Chemical Fundamentals, Modeling and Simulations, Experiments, Pollutant Formation*. - Berlin: Springer, 2001.
2. 18th World Hydrogen Energy Conf., 17-19 May 2010, Essen, Germany. <http://www.whec2010.com>
3. Ni M., Leung D.Y.C., Leung M.K.H. A review on reforming bio-ethanol for hydrogen production // *Int. J. Hydrogen Energy*. - 2007. - **32**. - P. 3238-3247.
4. Deminsky M., Jivotov V., Potapkin B., Rusanov V. Plasma-assisted production of hydrogen from hydrocarbons // *Pure Appl. Chem.* - 2002. - **74**, N 3. - P. 413-418.
5. Bromberg L., Cohn D.R., Rabinovich A., Nadidi K., Alexeev N., Samokhin A. Plasma catalytic reforming of biofuels // MIT Plasma Sci. Fusion Center, Cambridge, MA, Report PSFC/JA-03-28. - 2003. Available <http://www.psf.mit.edu>
6. Petitpas G., Rollier J.-D., Darmon A., Gonzales-Aguilar J., Metkemeijer R., Fulcheri L. A comparative study of non-thermal plasma assisted reforming technologies // *Int. J. Hydrogen Energy*. - 2007. - **32**. - P. 2848-2867.
7. Fridman A. *Plasma Chemistry*. - N.Y.: Cambridge Univ. Press, 2008.
8. Fridman A., Kennedy L. *Plasma Physics & Engineering*. - N.Y.: Taylor & Francis, 2004.
9. Buchnev V.V., Koval S.D., Chernyak V.Ya. Nonequilibrium arc plasma in transverse air flow // *Bull. Univ. of Kyiv: Series: Phys. & Math.* - 2000. - N 1. - P. 315-319.
10. Chernyak V.Ya., Naumov V.V., Yukhymenko V.V., Babich I.L., Zrazhevskyy V.A., Voevoda Yu.V., Pashko T.V. Arc discharge in a cross flow of gas // *Probl. Atom. Sci. Technol., Ser. Plasma Phys.* - 2005. - **11**, N 2. - P. 164-166.
11. Yukhymenko V.V., Chernyak V.Ya., Naumov V.V., Veremii Iu.P., Zrazhevskij V.A. Combustion of ethanol + air mixture supported by transverse arc plasma // *Probl. Atom. Sci. Technol., Ser. Plasma Phys.* - 2007. - **13**, N 1. - P. 142-144.
12. Yukhymenko V.V., Chernyak V.Ya., Naumov V.V., Prisyazhnevych I.V., Skalny J.D., Matecic S., Sabo M. Optical researches of discharge plasma in air channel with water wall // *Bull. Univ. of Kyiv: Series: Phys. & Math.* - 2006. - N 6. - P. 346-353.
13. Veremii Iu.P., Chernyak V.Ya., Trokhymchuck A.K., Kondratyuk Ya.V., Zrazhevskij V.A. Physicochemical properties of a plasma-liquid system with an electric discharge in a gas channel with a liquid wall // *Ukr. J. Phys.* - 2006. - **51**, N 8. - P. 769-774.
14. Veremii Yu. P., Chernyak V. Ya., Naumov V.V., Yukhymenko V.V., Dudko N.V., Optical properties and some applications of plasma-liquid system with discharge in the gas channel with liquid wall // *Probl. Atom. Sci. Technol, Ser. Plasma Phys.* - 2006. - **12**, N 6. - P. 216-218.
15. Chernyak V.Ya, Yukhymenko V.V., Slyusarenko Y.I. Conversion of ethanol in plasma of the gas discharge with liquid walls // *Bull. Univ. of Kyiv. Series: Phys. & Math.* - 2007. - N 1. - P. 292-295.
16. Chernyak V.Ya., Yukhymenko V.V., Slyusarenko Y.I., Solomenko E., Olshevskii S.V., Prisyazhnevich I.V., Naumov V.V., Lukyanchikov V., Demchina V.P., Kudryavtsev V.S. Plasma conversion of ethanol // *Ind. Heat Eng.* - 2007. - **29**, N 7. - P. 165-169.
17. Velikodnyi V., Berkova M., Vorotinin V., Grishin V., Kruchenko O., Popov V., Rychagov E., Polotnyuk O., Bykov A., Dobryneths Ya., Tolkunov B. Application of volumetric-diffusion discharge in microporous liquid for purification waste water in civil live and industry. *Intern. Conf. "Energy Efficiency-2007"*, 15-17 Oct. 2007, Kyiv, Ukraine. - Abstracts. - 2007. - P. 91-93.
18. Spectrum Analyzer. Available: <http://www.physics.muni.cz/~zdenek/span/> / Z. Navratil, D. Trunek, R. Smid, L. Lazar. A software for optical emission spectroscopy – problem formulation and application to plasma diagnostics // *Czechoslovak J. Phys.* **56**, Suppl. B. – 2006. - P. 944-951.

19. SPECAIR. Available: <http://www.specair-radiation.net> / C. O. Laux, T. G. Spence, C. H. Kruger, and R. N. Zare. Optical diagnostics of atmospheric pressure air plasma // *Plasma Sources Sci. Technol.* 12, no. 2, pp. 125-138, 2003.
20. Levin D.A., Laux C.O., Kruger C.H. A general model for the spectral calculation of OH radiation in the ultraviolet // *J. Quant. Spectrosc. Radiat. Transfer.* - 1999. - **61**, N 3. - P. 377-392.
21. Laux C.O., Spence T.G., Kruger C.H., Zare R.N. Optical diagnostics of atmospheric pressure air plasmas // *Plasma Sources Sci. Technol.* - 2003. - **12**. - P. 125-138.
22. Raizer Yu.P. *Gas Discharge Physics.* - Berlin: Springer-Verlag, 1997.
23. Shchedrin A. I., Levko D.S., Chernyak V.Ya., Yukhymenko V.V., Naumov V.V. Effect of air on the concentration of molecular hydrogen in the conversion of ethanol by a non-equilibrium gas-discharge plasma // *JETP Lett.* - 2008. - **88**, N 2. - P. 99-102.
24. A.Shchedrin 's group Web site. Available: <http://www.iop.kiev.ua/~plasmachemgroup>
25. NIST Standard Reference Databases Online. Available: <http://www.nist.gov/srd/>
26. Frenkel Ya.I. *Kinetic theory of liquids.* - Moscow: Nauka, 1975.
27. Chernyak V.Ya., Yukhymenko V.V., Solomenko E.V., Slyusarenko Yu.I., Olzhevskij S.V., Prisyazhnevich I.V., Martysh E.V., Naumov V.V., Demchina V.P., Kudryavtsev V.S. Plasma production of hydrogen-enriched gases from ethanol // *Proc. 3rd Int. Workshop & Exhibit. Plasma Assisted Combustion*, 18-21 Sept. 2007, Falls Church, Virginia, USA /Ed. I. Matveev. – APT. - 2007. - pp. 33-36.
28. Chernyak V.Ya., Olszewskii S.V., Yukhymenko V.V., Prysiazhnevych I.V., Verovchuk M.A., Solomenko E.V., Zrazhevsij V.A., Naumov V.V., Shchedrin A.I., Levko D.S., Demchina V.P., Kudryavtsev V.S. Study of plasma conversion of ethanol into syngas in dynamic plasma-liquid systems // *Proc. 4th Int. Workshop & Exhibit. Plasma Assisted Combustion*, 16-19 Sept. 2008, Falls Church, Virginia, USA /Ed. I. Matveev. – APT. - 2008. - pp. 68-70.

LIST OF ABBREVIATIONS

EOARD – European Office of Aerospace Research and Development

STCU – Science and Technology Center of Ukraine

KNU – Kyiv National Taras Shevchenko University

PLS – plasma-liquid system

DGCLW – discharge in the gas channel with liquid wall

BTA – blowing transverse arc

DC – direct current

AC – alternating current

OES – optical emission spectroscopy

NIR – near infrared

UV – ultraviolet

US – ultrasound

SAS - surface-active substance

SINGAS – synthesis gas containing hydrogen H₂ and carbon monoxide CO